

---

## Project Report

### **Seismic response of vertical post-tensioned connection for modular steel structures**

---

**Submitted by**

Ayush Agrawal

Roll No. 170100044

Department of Mechanical Engineering

IIT Bombay

**Supervised by**

Prof. Oya Mercan

Associate Professor

Department of Civil and Mineral Engineering



**University of Toronto**  
**MITACS Globalink Research Internship**

# *Simulation #1*

## *Seismic Evaluation of R4W*

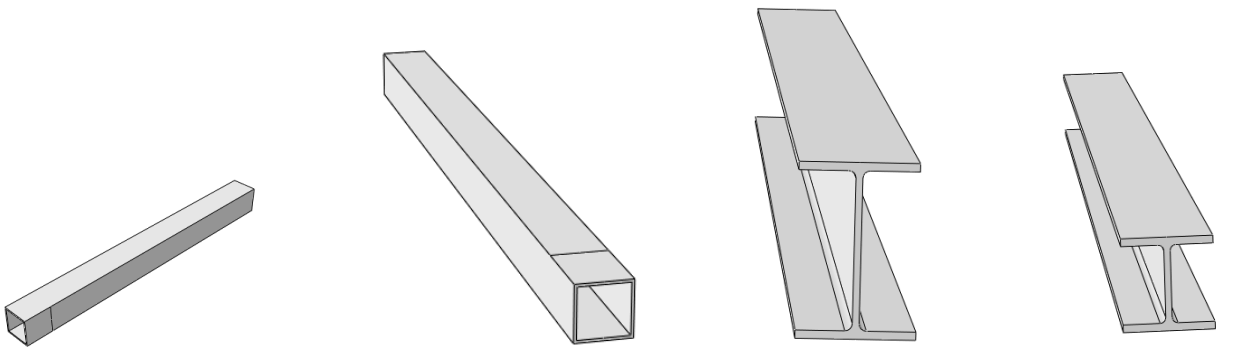
This report contains the details about modelling and simulation of R4W structure. The structure was modelled in ABAQUS using 3D solid elements mainly Wide Flange Beams and HSS Columns. The data obtained from coupon test of these structural elements was used to generate bilinear model of the materials out of which these structural elements were fabricated. In the experimental setup these beams and columns were connected through welding. This makes it necessary to model weld and assign appropriate material to it in order to obtain similar results as that of the experimental ones. A hydraulic actuator imposed quasi-static cyclic displacement; with slow displacement rates; in accordance with the ASCI protocol. Hysteresis and skeleton curves will be reported for the R4W specimen. The report concludes with a discussion on details that can be the sources of error along with possible ways of reducing computational time taken to solve the problem numerically.

## **1 Details of Beams and Columns constituting R4W**

R4W is a part modular steel structure in which all sides of the upper column were welded to the bottom column. Wide flange beams were further welded to these HSS columns to form R4W. In ABAQUS, three dimensional solid homogeneous elements were used to model these beams and columns.

Cross Sectional Properties of Structural Elements	
Columns and Beams	Cross Sectional Properties
Floor Beam	W 150 × 18 (Flange) W 150 × 18 (Web)
Ceiling Beam	W 100 × 19 (Flange) W 100 × 19 (Web)
Columns	HSS 127 × 127 × 6.4

The exact dimension of these wide flange beams can be found on [AmesWeb](#).



(a) Bottom Column

(b) Upper column

(c) Floor Beam

(d) Ceiling Beam

Partitions were created to facilitate the process of assembly. Also, creating partitions was necessary because web and flange of the beams have different material properties as revealed in the coupon test.

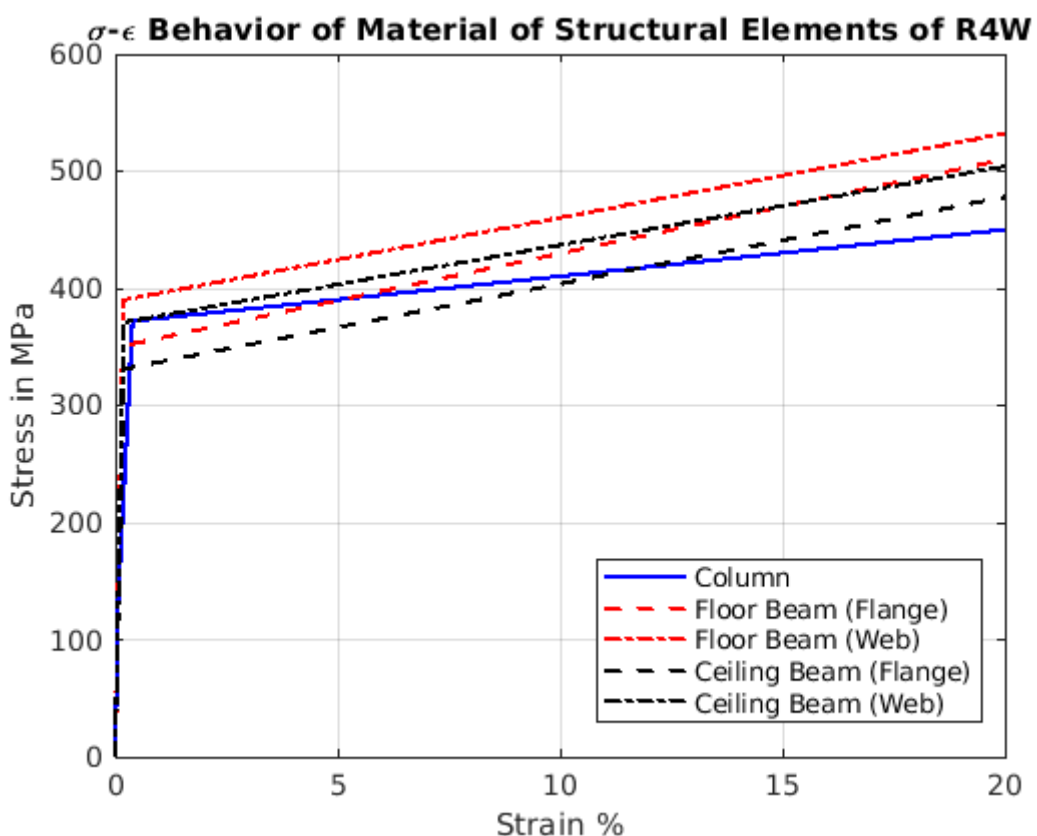
## 2 Material Properties of Beams and Columns

The steel beams were produced from ASTM A572 Gr50, and the columns were made from CSA G40.21-350 W Class C. Coupon tests were conducted to derive the stress strain behaviour of material used in fabrication of elements. The data obtained about the yield point and ultimate point was used to generate the bilinear stress strain model of the materials involved.

In ABAQUS, elasto-plastic behavior was created using the data given in the table below.

Material properties of the structural elements				
Elements	E (MPa)	$f_y$ (MPa)	$\epsilon_y$ (%)	$f_u$ (MPa)
Column	193,350	372	0.39	450
Floor Beam (Flange)	193,652	351	0.20	510
Floor Beam (Web)	197,463	390	0.19	532
Ceiling Beam (Flange)	202,247	331	0.19	478
Ceiling Beam (Web)	196,213	371	0.19	574

The strain at ultimate point was taken to be 20%. Also, the average elastic limit strain (proportional or linear limit strain) for the column coupons were 0.07%. The data for elastic limit point, yield point and ultimate point was used to model the material for columns. For modelling the material for beams only yield and ultimate point were used.



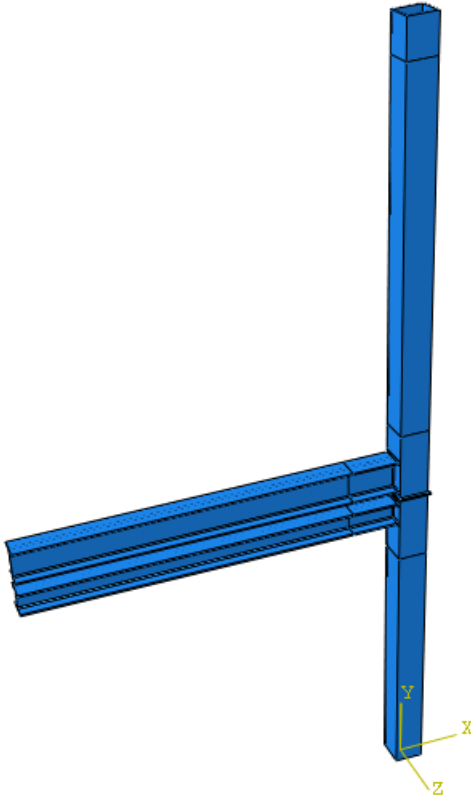
### 3 Modelling weld joint and Assembly

During experimentation, elements were fillet welded together to form the structural setup. This means that the stresses among the elements were transferred via welded joints. Therefore it will be incorrect to not consider weld joint in the model and use only tie constrain between the connecting elements of the structure.

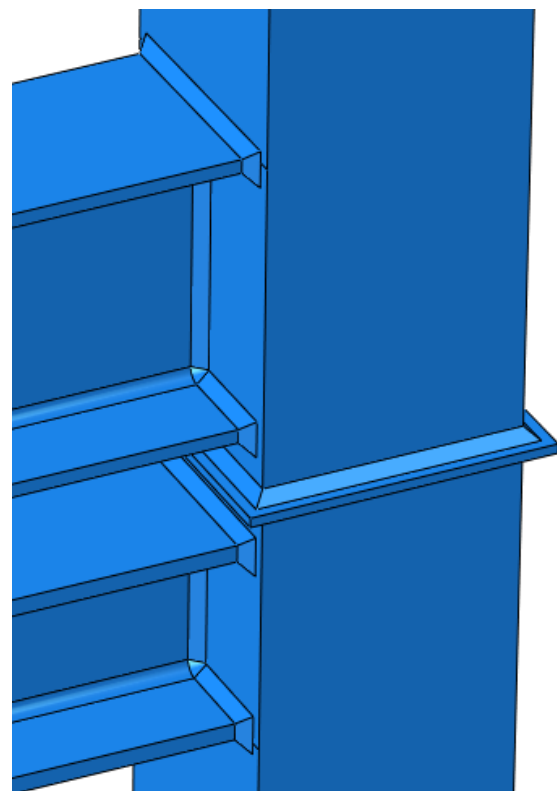
In order to weld joint in ABAQUS, we need to merge the assembled parts. Merging the elements will create another part which is nothing but R4W structure. Once the desired structure is created, **camfer** can be created at the edges where weld joint is needed. Here the weld joint was there between Floor beam and Upper column , Upper column and Bottom column ;and Bottom column and Ceiling beam. One thing should be noted that without merging the elements camfer cannot be created. This is because without merging, the edge at which we want to create camfer will be shared by two solid objects, mathematically this is called a manifold edge at which ABAQUS does not allow to generate camfer. The dimension of the camfer used in this analysis was **6 mm**. More details about modelling can be obtained from [thesis](#) by Kyle J. Tousignant.

Once the assembly is complete, with proper weld joints at desired locations, appropriate partitions should be made for section assignments where we need to assign appropriate material to the parted section. In our case, we have done coupon test to take out data for material behaviour. We can use this data to model our own material and assign it to appropriate sections.

Since we want the load to get transferred only through the weld joint, we need to assign **seam crack** to the surfaces through which the load is not going to be transferred. Upper columns and bottom column were joined together through welding and so in the model a weld plate was used in between the columns to generate the weld joint as shown in the figure below. The dimensions of the structural elements are given in the [paper](#) about Experimental investigations of vertical post-tensioned connection for modular steel structures. The dimension of the weld plate used was  $145 \times 145 \times 5$  and it is assigned the same material as that of the columns



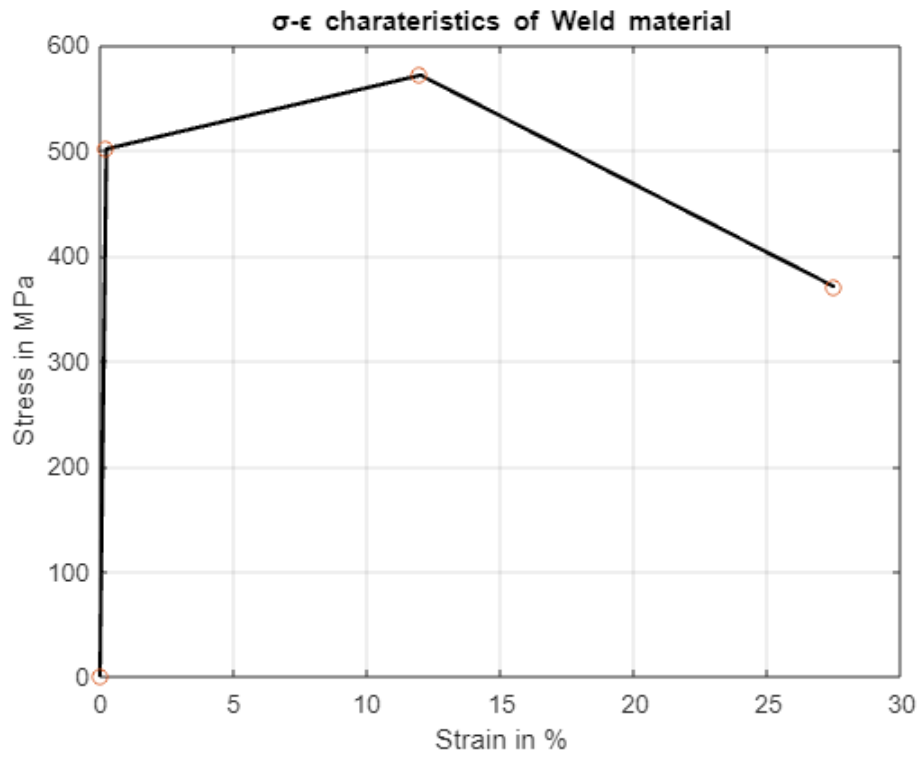
(e) Model of R4W



(f) Camfer used for modelling weld joint

Material properties of weld joint	
Properties	Value
Elastic Modulus	207,000 MPa
Yield Stress	501 MPa
Strain at yield point	0.24%
Ultimate stress	571 MPa
Strain at ultimate point	12.5%
Stress at Fracture point	370 MPa
Strain at Fracture point	27.5%

The stress strain characteristics of the weld material based on above data is shown below.



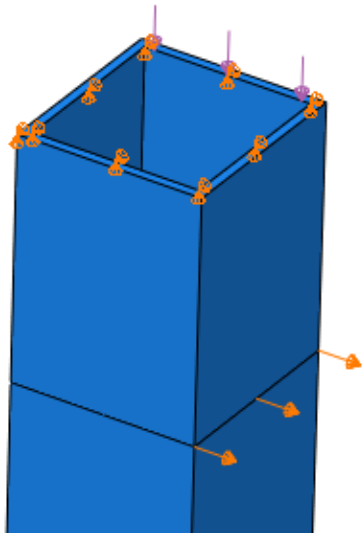
## 4 Boundary Conditions and loading

Boundary condition were imposed at the top face of upper column, bottom face of bottom column and left faces of both the I beams. At these boundaries rotation about all axis is permitted.

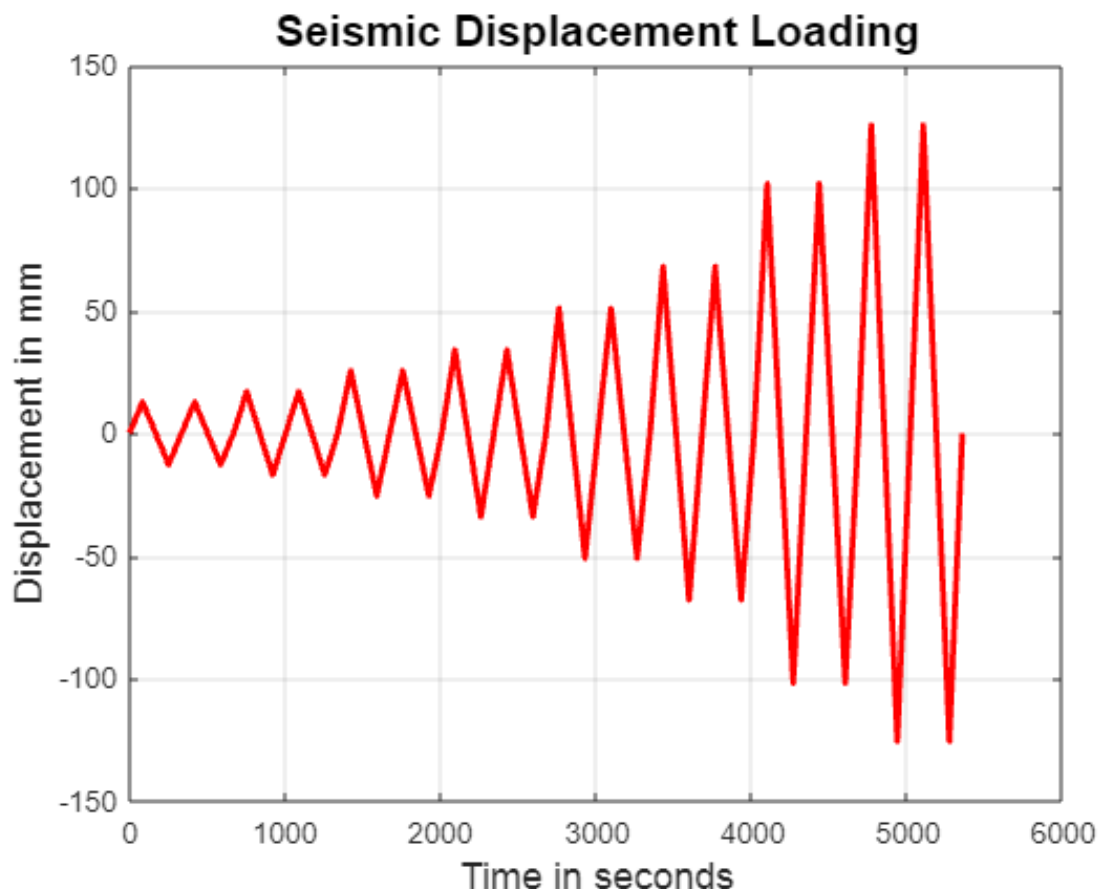
Translational motion restriction at boundary conditions	
Boundaries	Translational motion is restricted along
Top face of Upper column	y and z direction
Bottom face of bottom column	x, y and z direction
Left face of Floor Beam	y and z direction
Left face of Ceiling Beam	y and z direction

A load of 100kN is imposed at the upper face of the upper column. This load represents the vertical loads acting in the column of the first floor of the building and it was computed assuming a typical floor system comprised of concrete floor and steel deck (2.0 kN/m<sup>2</sup>) and insulation (0.25 kN/m<sup>2</sup>).

Superimposed dead loads for floors, roof, and ceilings are 0.75, 0.32, and 0.7 kN/m<sup>2</sup>, respectively. Live load of 1.9 kN/m<sup>2</sup> is considered in every floor and the snow load of 1.1 kN/m<sup>2</sup> is considered for the roof. For the seismic evaluation of R4W, a quasi-static cyclic loading in accordance with the ASCI protocol was imposed by a hydraulic actuator. The rate of displacement of the applied motion was 1.5mm/sec. The cyclic displacement load is applied at the right hand face of the upper column and the variation of imposed displacement can be seen below.



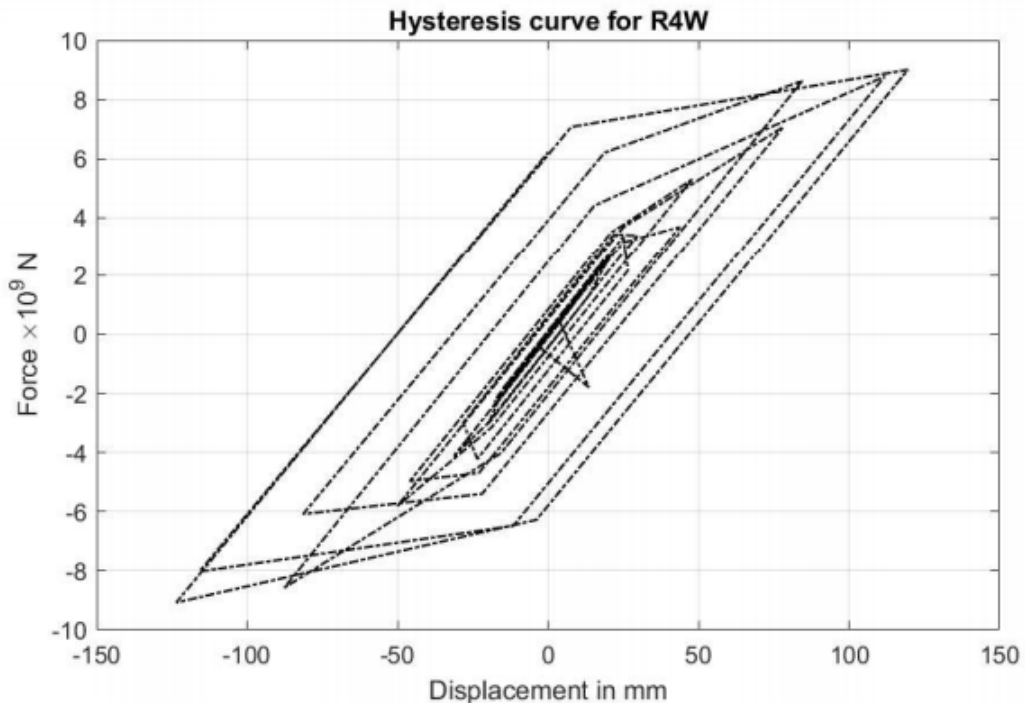
(g) Axial load and Cyclic Displacement load  
at upper column



It can be observed that number of cycles in set 1,2,3 and 4 are 2. As per the ASCI protocol the number of cycles should be 6,6,6 and 4 respectively. The number of cycles has been reduced in order to reduce the computation time. Doing this has reduced the time period of the problem from 10035 seconds to 5350 seconds.

## 5 Results

The hysteresis curve for the R4W structure is shown below. The curve is plotted between the force applied and the displacement that occurred at the point of loading.



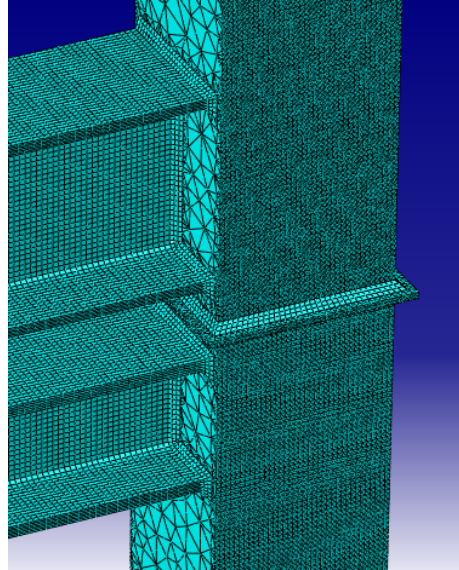
It can be noticed that the order of magnitude of force is  $10^9$  N. This could be a problem that occurred due to inconsistency in the specification of physical properties of the materials (the properties given were of the order of  $10^9$  Pa. The order of force would be correct if the properties were given in MPa).

The difference between this numerical and experimental hysteresis curve can be observed visually. One of the difference is that maximum force applied in simulation was 9.004 units while in experiments the maximum force was nearly 15 units. The reason behind this could be missing friction force between surfaces in the simulation. This observation asks for the need of modelling friction contact surfaces between structural elements. Another difference between experimental and numerical results was that, in experiments there was a crack in the weld between floor beam and upper column but in the numerical model the crack was observed in the weld joint between ceiling beam and bottom column.

The data for time dependent displacement load applied at upper column and the corresponding reaction force at the point point of application of load can be obtained from [Hysteresis\\_Data\\_R4W](#).

## 6 Possible errors and Scope of improvement in Modelling

1. In this simulation, 3D solid homogeneous models were used. Meshing these solid parts in the assembly created around  $3 \times 10^5$  nodes in the model. Because of this it took days to solve the problem. In further simulation shell models would be considered in place of solids as this will reduce the number of nodes to great extent resulting in lesser computational time. Additional features like weld plate used in this model might not be used to reduce the additional mesh elements.



(i) Local Mesh around melded region

2. While modelling the materials in ABAQUS, bilinear models were used. In further simulations data obtained from the coupon tests might be used to model the near exact stress strain behavior of the material constituting the structural elements.
3. Also there were certain problems while creating seam cracks. Creating seam cracks will render some regions unmeshable. For these regions tetrahedral mesh has to be created that can vary significantly in size and density across the same region. This can be rectified by creating a clearance between the two surfaces which need to be connected by weld joint. But in this case ABAQUS will not allow us to make a camfer. This issue need to be rectified in order to rule out the problem that is experienced during meshing after seam is assigned.

# ***Seismic Evaluation of R4W***

## *Improving the model*

This report contains the information about changes that were made in the simulation to improve the numerical results for the seismic behavior of R4W. The changes not only improved the results but also reduced the computational time required to complete the analysis. The stress fields and other necessary observations were found to be in accordance with those observed during experimentation. Even if the numerical and experimental results match qualitatively, it is important that they resemble each other quantitatively as well.

In order to obtain the results shown in this report, four simulations were performed. These four simulations were performed in ABAQUS/Standard which is used to perform static simulations. Since our problem is a quasi-static problem, choosing this environment wasn't wrong. But it was observed that all the four simulations were aborted because of large plastic deformation in structure. These errors will be discussed further in this report.

It has been mentioned what this report is going to focus on, the details regarding dimension of structural elements, their material and assembly will not be given.

## **1 Mistakes in the last simulation**

Several errors were found in the last simulation. These are mentioned below along with the affects they made on the results.

1. In ABAQUS, while doing the simulation one has to be consistent with the units while modelling the problem because the software does not allow the user to mention the units.

Consistent units in ABAQUS		
Quantity	SI	SI(mm)
Length	m	mm
Force	N	N
Mass	kg	tonne ( $\times 10^3 kg$ )
Time	s	s
Stress	$Pa(N/m^2)$	$MPa(N/mm^2)$

In the simulation done earlier, SI(mm) was used but the stresses mentioned while modelling the materials were given in Pa. This increased the order of magnitude of the forces reported previously from  $\times 10^3$  N to  $\times 10^9$  N.

2. In the last simulation a mid plate was used to model the weld connection between upper and bottom column. This made the connection more stiffer than can increase the force required to generate the desired displacement.
3. The boundary conditions that were given to the last model were correct with respect to the translational and rotational freedom, but the regions that were selected for the boundary conditions were incorrect. Surfaces were selected where these boundary conditions made. Selecting a surface and restricting motion in x and y direction will constraint all the points such that rotation along

*z*-direction will be restricted. This also made the problem over constrained and might have altered the value of forces required to create the desired displacement. This error was found at all the four regions where boundary conditions were specified.

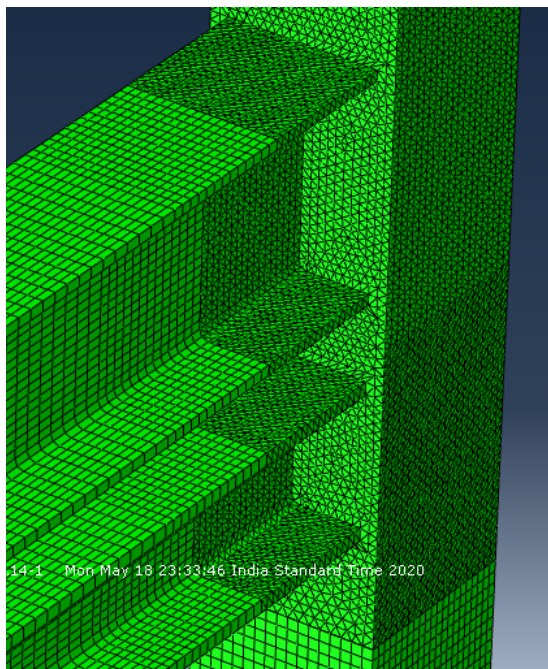
4. The meshing created in the last model was excessively fine. There were total  $3.3 \times 10^5$  mesh elements in the structure. This made the analysis to go on for around **90 hours**.

5. The stress obtained from the numerical model was different from that observed during the experiments. The reason behind this was the incorrect boundary condition that were made in the model. In the experiments high strain were observed for the floor beam but in last model the same was seen for the ceiling beam which was incorrect.

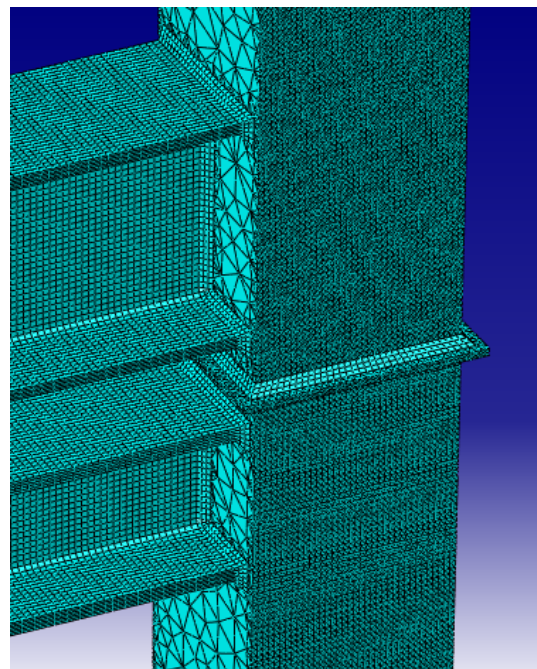
## 2 Improving the mesh and Boundary conditions

Making a fine mesh throughout the model thinking that results obtained will be more accurate, is not a good idea as it will drastically increase the computation time and it is possible that job get aborted because the system requires many time increment to complete the analysis.

In order to reduce the computation time ( $3.3 \times 10^5$  elements took approximately 90 hours to solve) the number of elements in the model were reduced to comparatively small number. At the region of interest, i.e. about the weld, fine tetrahedral (C3D10) mesh was used with a size of 8mm. The mesh was made coarser with cubical elements (C3D8R) as we move away from this region towards the boundaries. To do this one can use biasing or make partitions where the edges can be seeded into create elements of desired size. In further simulations the latter technique was used for meshing. Once all the edges were seeded, global mesh was created. This generated  $5.8 \times 10^4$  mesh elements in the model. The mesh generated was very structured in all the regions and fine around the weld. One thing that should be taken care of is that meshing should be done once all the interaction in the model were made. In our case we need to assign seams cracks in the region enclosed by the weld as we want the load to get transferred only through the weld. With this new mesh, the computation time was less than **2 hours** for an analysis with **time period = 5931 seconds**.



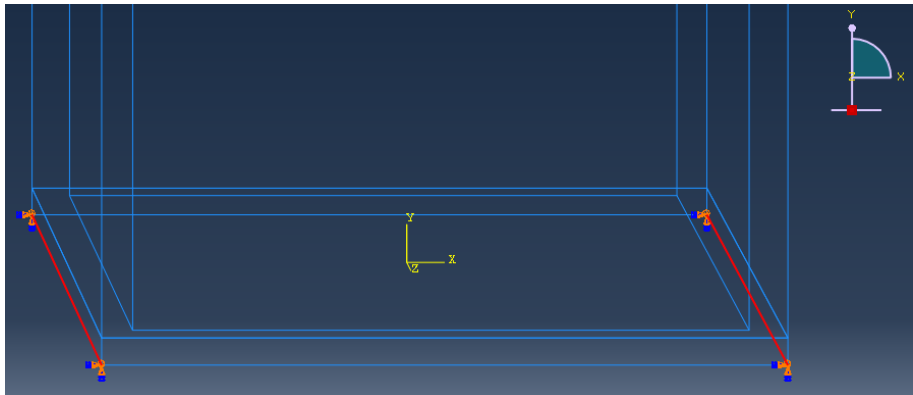
(a) Meshing in new model



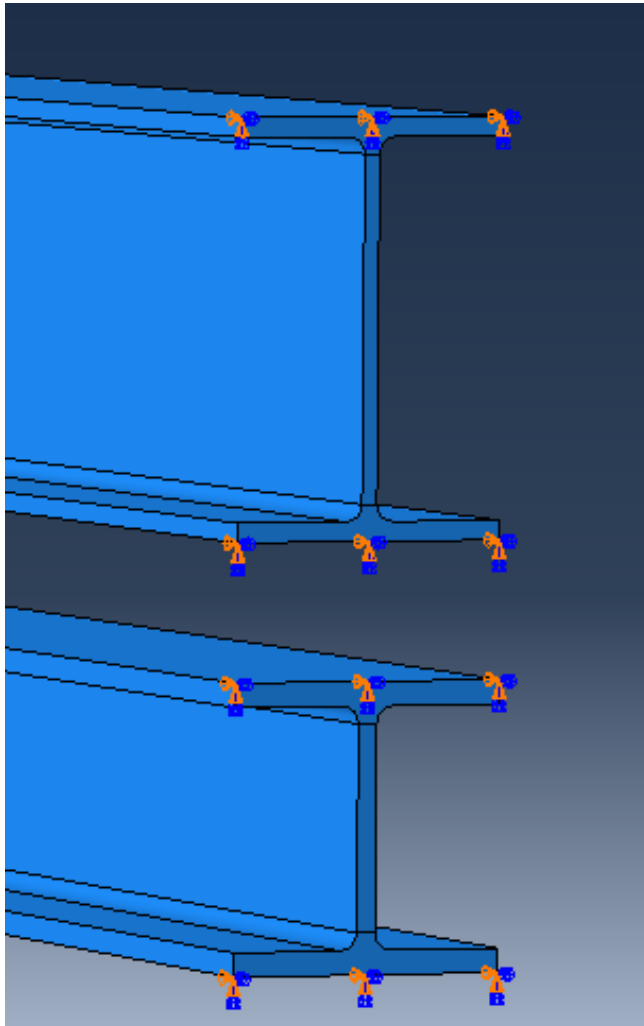
(b) Meshing in previous model

As it was mentioned in the previous section that there was a mistake in assigning boundary condition to the problem. The problem was that the rotation at the boundaries were restricted. This was rectified in the subsequent simulations by choosing edges and points instead of surfaces for assigning boundary conditions.

Some changes were also made to the behavior of the material. In the last simulation isotropic hardening for the material was used but in recent simulation kinematic hardening was used.



(c) Boundary condition at bottom face of the lower beam assigned to the edges



(d) Boundary condition at the end of floor and ceiling beam assigned to edges

### 3 Errors that lead to termination of the analysis

It was mentioned earlier that 4 simulation were done this time to obtain better results. All of these simulation were terminated because of the following reasons:

**Simulation 1** - Time period for which analysis was done is 1340 out of 3000 seconds. Results were obtained only for the first 2 sets of the cyclic load.

The simulation was aborted with these errors:

"THE STRAIN WAS SO LARGE THAT ABAQUS WILL NOT ATTEMPT PLASTICITY CALCULATION AT \_\_\_ POINTS"

"EXCESSIVE DISTORTION AT \_\_\_ POINTS IN (CONTINUUM) ASSEMBLY"

For this simulation the displacement load used had very less data points, only the peak values were given in the data. This data was created and for every set of the cycle the displacement rate was 1.5mm/sec. This means there were sudden jumps in the data. For this ABAQUS has to make interpolations which leads to slow computations and these kinds of errors may also arise. In order to tackle this in next simulation large data with several data points was used (experimental data was used for the simulation purpose). This actually helped in reducing the computation time and gave better results in terms of completion of larger part of the analysis.

**Simulation 2** - Time period for which the analysis was done is 1760 out of 5406.4 seconds. For this simulation experimental data was used with some changes made to the last set of the laod. Results were obtained for the first 4 sets of the cyclic load.

The simulation was aborted with these errors:

"FORCE EQUILIBRIUM NOT ACHIEVED"

(A necessary condition that should be met in ABAQUS/Standard)

The reason why this error occurred was the high displacement rate (2mm/sec - experimental value) in the 5,6,7 and 8th set of the displacement load. Once there is a large deformation in the structure along with high displacement rates the problem loses its static nature. To prevent this error from occurring in further simulations the displacement rate for all sets of the cyclic load except the last (3.7% drift) was 0.5 mm/sec and for the last set it was 1mm/sec. This alteration in the data helped in achieving equilibrium at all points during the analysis.

**Simulation 3** - Time period for which the analysis was done is 2700 out of 5931 seconds. For this simulation only 2 cycles per set was taken in order to limit the total time period of the load. Results were obtained for the first 5 sets along with the first cycle of 6th set of the cyclic load.

The simulation was aborted with these errors:

"THE STRAIN WAS SO LARGE THAT ABAQUS WILL NOT ATTEMPT PLASTICITY CALCULATION AT \_\_\_ POINTS"

"EXCESSIVE DISTORTION AT \_\_\_ POINTS IN (CONTINUUM) ASSEMBLY"

This time the error occurred for less number of points because in this simulation the meshing near weld and the boundary condition at the bottom of the lower beam was made much more finer ( $1.3 \times 10^5$  elements were used). This was done because these were the regions where high plastic deformations were found. It was also found that the plastic strain was excessively large at the bottom of the lower beam.

**Simulation 4** - Time period for which the analysis was done is 5400 out of 5931 seconds. Results were obtained for the first 7 sets along with the first cycle of 8th set of the cyclic load.

The simulation was aborted with these errors:

"THE STRAIN WAS SO LARGE THAT ABAQUS WILL NOT ATTEMPT PLASTICITY CALCULATION AT \_\_\_ POINTS"

"EXCESSIVE DISTORTION AT \_\_\_ POINTS IN (CONTINUUM) ASSEMBLY"

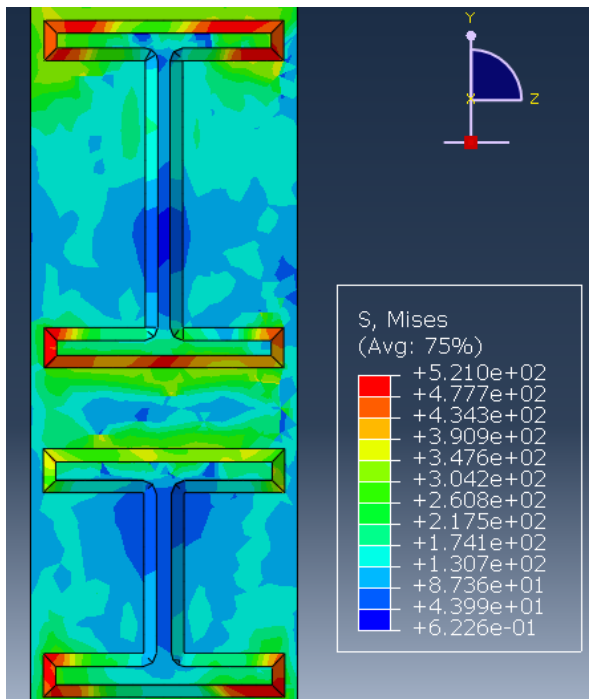
It can be observed that there has been a significant improvement in the time for which analysis was done. There were several changes that were made for this simulation. In this simulation number of mesh elements used were  $5.8 \times 10^4$ . Now the first change that was made was that a plate (Cross section - 127mm  $\times$  127mm and thickness - 5mm) made up of the same material as that of the column was attached at the bottom of the lower column. In this plate very fine mesh of dimension 5mm was used. The boundary condition was provided at the bottom surface of the plate. This was done because smaller the element smaller is the distortion. Along with this mesh control was also applied to the model which provided the option of distortion control. But in ABAQUS/Standard, distortion control can be given only to the tetrahedral elements in the elements. The effect of distortion control on the results will be discussed in further sections. Along with distortion control, enhanced [hourglass control](#) was used which provides improved coarse mesh accuracy with slightly higher computational cost and performs better for nonlinear material response at high strain levels when compared with the default total stiffness formulation. All these changes and controls helped in getting better results but still there is a scope improving the model which will be discussed further sections.

## 4 Results

In this section results from the 4<sup>th</sup> simulation will be displayed. In this simulation analysis was completed upto first cycle of 8<sup>th</sup> set of the seismic load. A comparison will also be reported which shows the effect of distortion control on the results obtained. The difference was seen between the plastic strain fields around weld region in simulation 3 and 4.

### 4.1 Stress Fields

In the last report no comments about the stress field was made. Although in the last simulation the stress field around ceiling beam was more intense than floor beam which is an incorrect observation. The figure below shows the stress fields around the welded regions.

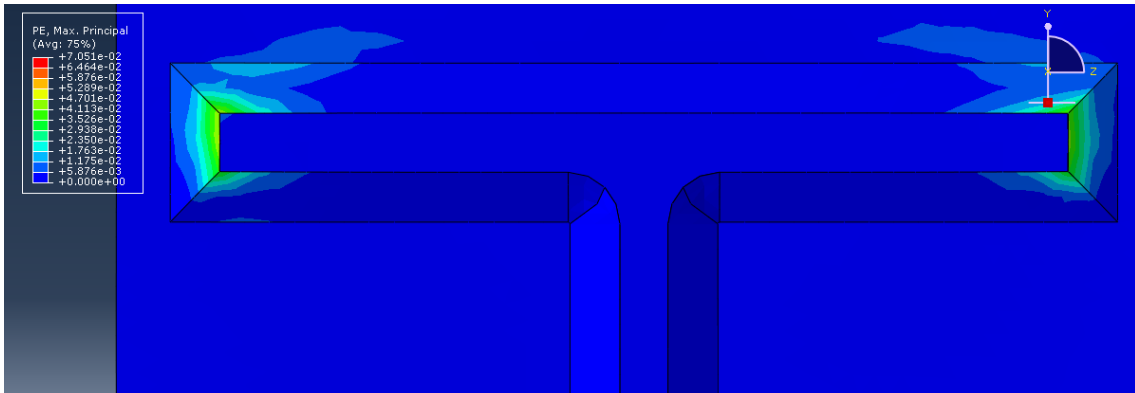


(e) Stress field around welded region in Simulation 4 (distortion control)

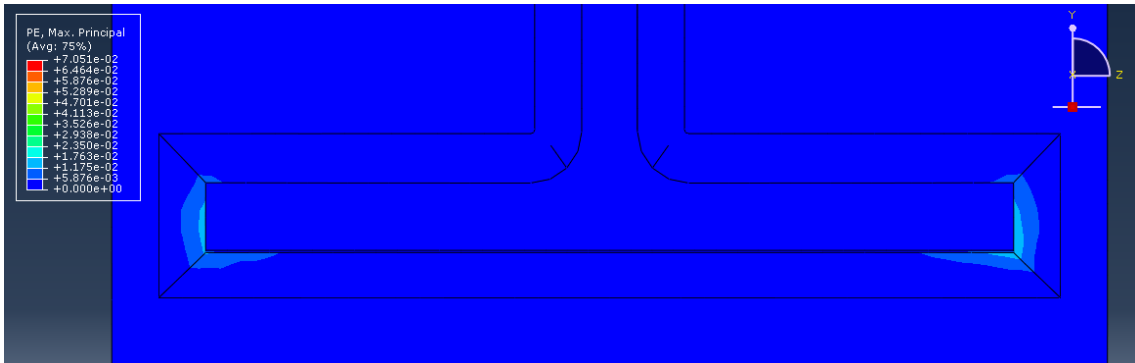
It should be noted that here the **floor and ceiling beam were erased** in post processing to give a better view of the stress field. It is worth observing that loads were transmitted through the weld as the stresses in weld are high as compared to the region they are enclosing. Please take a note of the stress value in weld region as it will be required in discussion about plastic strain fields.

## 4.2 Plastic Strain Fields

This quantity has been an important factor in the last few simulation as it decides whether our analysis will complete or will be terminated. We will take a look at the plastic strain fields around two region, one around the weld and other at the boundary condition at lower beam. These were the regions where high plastic strains were observed. The figures below display the strain field in weld at floor and ceiling beam.



(f) Plastic strain in weld at floor beam observed in Simulation 3



(g) Plastic strain in weld at ceiling beam observed in Simulation 3

It should be noted that plastic strain in weld high as compared to the nearby regions. This observation comes in agreement with the fracture that was observed during the experiment. Also the plastic strain in the ceiling beam weld is less than the floor beam weld.

Now lets have a look at the impact that distortion control had on the solution fields. It was observed that there was no impact on the stress fields but a significant impact was observed in the strain fields. This could be seen as in Simulation 3 where there was no distortion control, the plastic strain started to appear at 5<sup>th</sup> set of the cyclic load but in Simulation 4 where distortion control was applied, no plastic strain was observed even at the 8<sup>th</sup> set of the cyclic load. This can be observed in the figure below. Clearly, it is the effect of distortion control that prevented the elements in this region from deforming further.



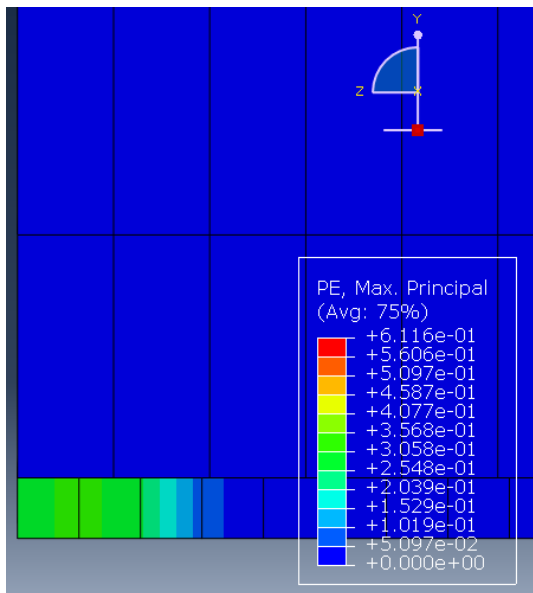
(h) Plastic Strain around welded region in Simulation 3 at 2%drift



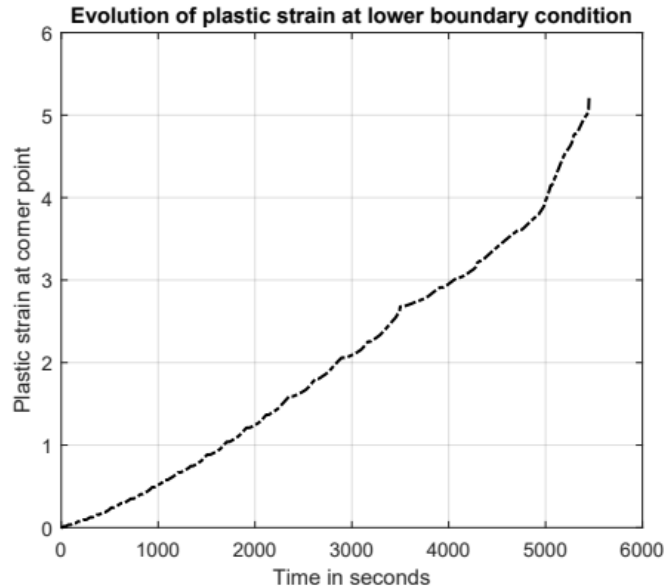
(i) Plastic Strain around welded region in Simulation 4 (distortion control) at 3.7%drift

As we have seen in previous section that most of our simulation were terminated because of excess plastic strain at significant number of points, we should have a look at how the plastic strain evolved at region of very high plastic strain like bottom face of lower column where boundary condition has been given.

It is evident from this curve that plastic strain at this region is very high. We need to assign distortion control in this region.



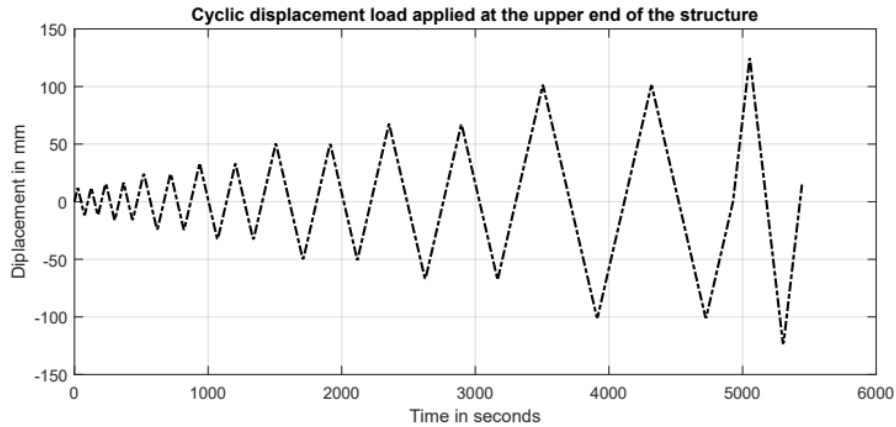
(j) Plastic Strain at corner point of bottom plate used in Simulation 4



(k) Evolution of plastic strain at this point

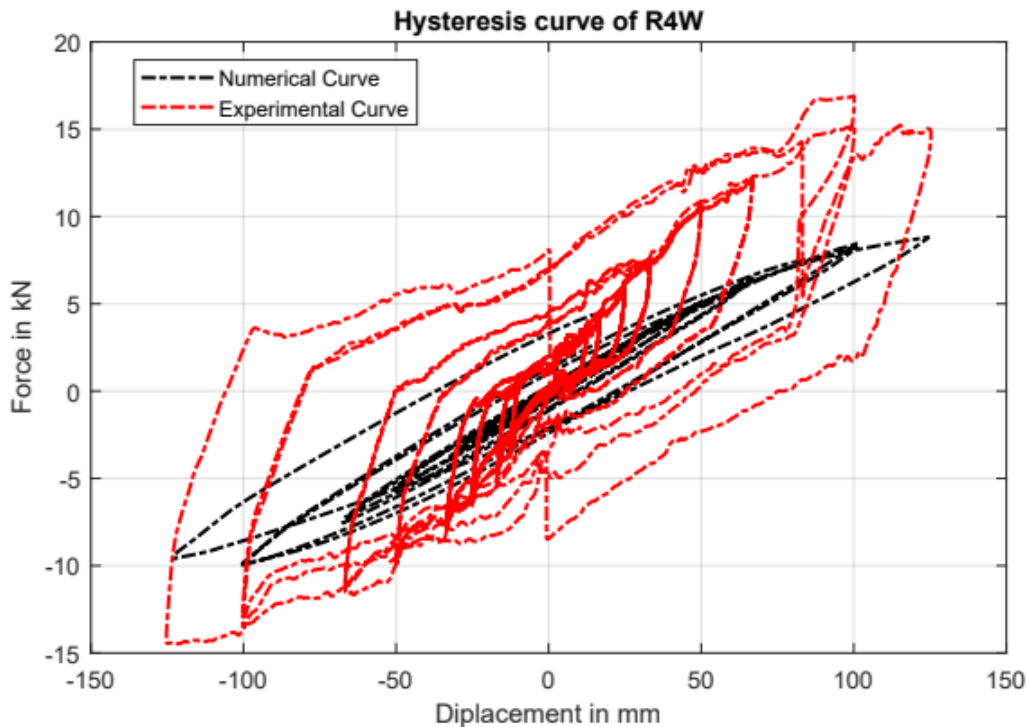
### 4.3 Displacement and Hysteresis Curve

The following graph shows the displacement that was recorded at the upper end of the structure. It can be seen that last cycle of the load is not present as the analysis was terminated due to excess plastic deformation at the lower end.



(l) Displacement recorded at upper end for 5400 seconds out of 5931 seconds

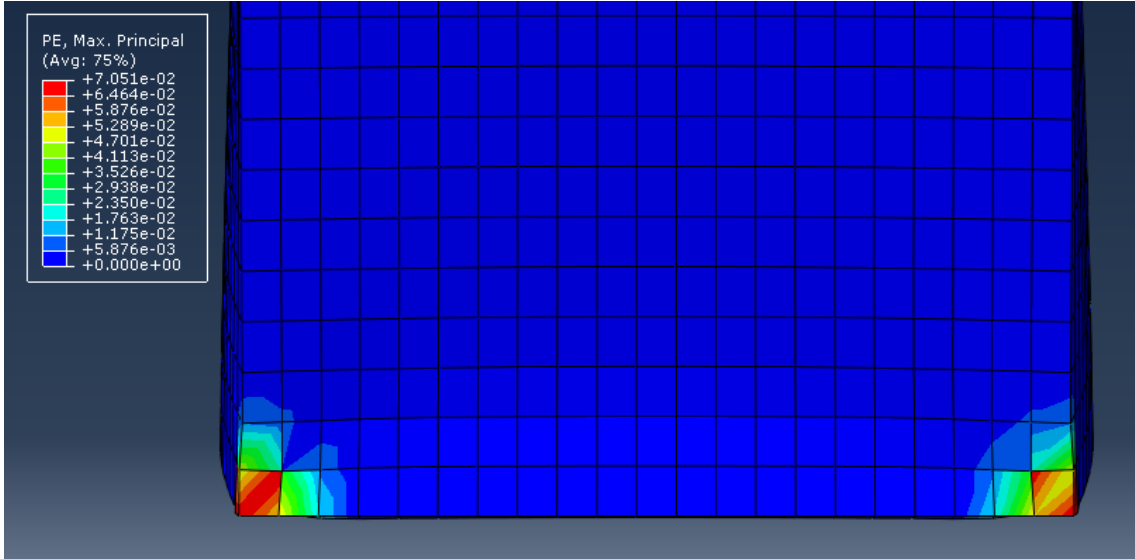
The next graph is a comparison between numerical hysteresis obtained from Simulation 4 and the experimental hysteresis. There are large differences between the two data. I think that this difference calls out for appropriate modelling of the material. In the experimental curve both kinematic and isotropic hardening can be seen. I think we need to model a combined hardening behavior for these materials. ABAQUS has the option of assigning combined hardening in materials.



(m) Comparison between Experimental and Numerical Results

## 5 Scope of improvement in Modelling

From the above sections it is clear that qualitatively numerical results and experimental results are same. All we need to do is to reduce the quantitative error between the two. In order to do this we need solve the problem of job termination due to excess plasticity in some regions. In our case this region is the boundary condition at bottom face of the lower column.



(n) High plastic strain at bottom face of lower column. The figure is from simulation 3 where the analysis was solved upto first cycle of 6<sup>th</sup> set of cyclic load. That's why the strain value has reached only 7%

This can be solved using distortion control by assigning appropriate [length ratio](#) to region of high plasticity. Such regions should be meshed using tetrahedral C3D10I elements only in ABAQUS/Standard. Although this technique was used in the fourth simulation, but in this distortion control was applied to the region around weld not to the region shown in the figure. It is because distortion control is not applicable to cubical (C3D8R) elements in ABAQUS/Standard. So, in further simulation we can try to mesh this region with tetrahedral mesh and assign proper distortion control to rule out the error. If this doesn't work then we can switch to quasi-static analysis in ABAQUS/Explicit where along with these control schemes we can use mass scaling to drastically reduce the computation time to minutes.

---

# *Seismic Evaluation of R4W*

## Simulation 5 and 6

This is a short report that contains the information about changes that were made in simulation 5 and 6 to improve the numerical results for the seismic behavior of R4W. These are the changes that were proposed in the last report. **Those proposals actually worked and Simulation 5 was successfully completed.** There were no errors related to high distortion and plasticity that were reported for the previous simulations.

In *Simulation 5*, some changes related to mesh and material were made. Here, **isotropic hardening** in material is used and the mesh at the bottom region of the lower column was made fine. As mentioned in the last section of the previous report, distortion control was applied at the bottom of the lower column where very high plastic strain was found. No distortion control was applied in the region around weld because it may affect the strain field in this region.

In *Simulation 6*, **kinematic hardening** in material was used for the purpose of comparing results with isotropic hardening used in Simulation 5.

## 1 Results from Simulation 5

### 1.1 Plastic Strain Fields

In the previous report the plastic strain around weld was shown. Due to applied distortion control in this region the plastic strain was zero. In this simulation distortion control was not applied to the region around weld and expected resulted were obtained. The figure below shows the plastic strain in welding of floor beam.

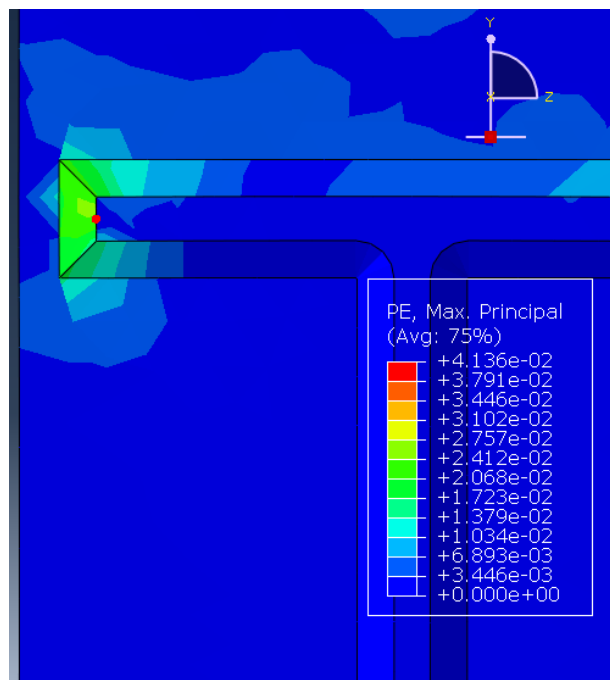


Figure 1: Plastic strain field in weld of floor beam

The point (The point lies in the weld region) highlighted in this figure recorded a maximum principal plastic strain of 5.4% and the maximum von Mises stress at the same point was 571 MPa. Also, the maximum von mises stress observed at weld of ceiling beam is 515MPa. The report does not include the stress field as it is the same as that obtained from Simulation 4. It can be referred from result section of the last report. These figures are for isotropic hardening. In Simulation 6, where kinematic hardening was used the maximum principal plastic strain in the floor beam weld region was 4.8% and the maximum von Mises stress was 532 MPa.

Let's have a look at points at the bottom of the lower column at which boundary condition have been applied. Although these points are extraneous from result point of view but because of the excess plastic strain seen at these points, it became necessary to analyse them. As it could be seen from the plot shown in the last report that the plastic strain at these points was around 500%, the region was modelled with distortion control with length ratio = 0.01. After this excess distortion was not observed at these points and the maximum principal plastic strain value at these points was 24.65% and maximum von Mises stress value recorded at these points was 450 MPa. It was observed that this stress value was constant for a large fraction of the time period of the analysis. This was the data from Simulation 5. In Simulation 6, the maximum von Mises stress at th same point was 468 MPa and the maximum principal plastic strain was 23.5%.

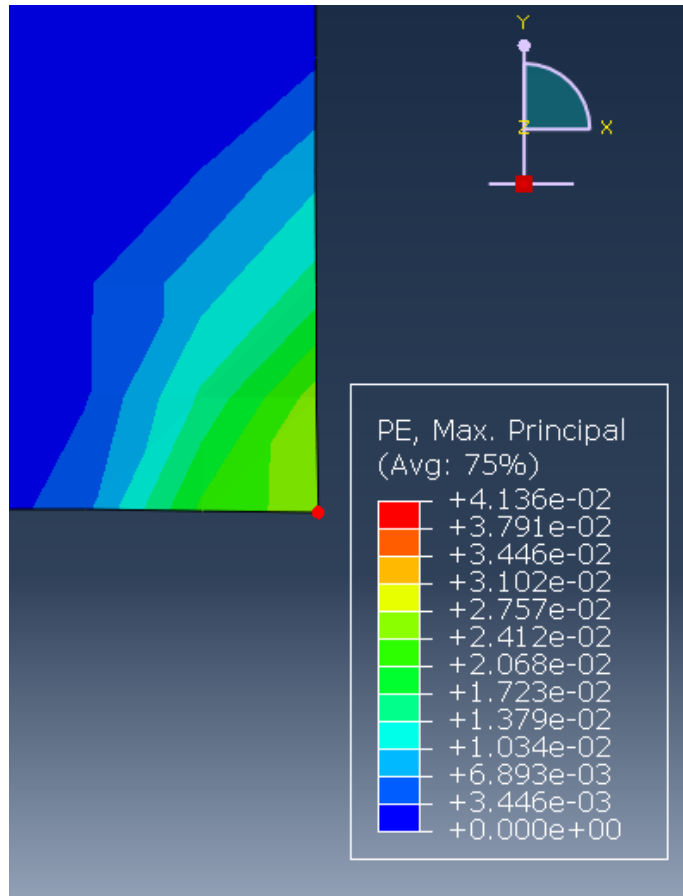
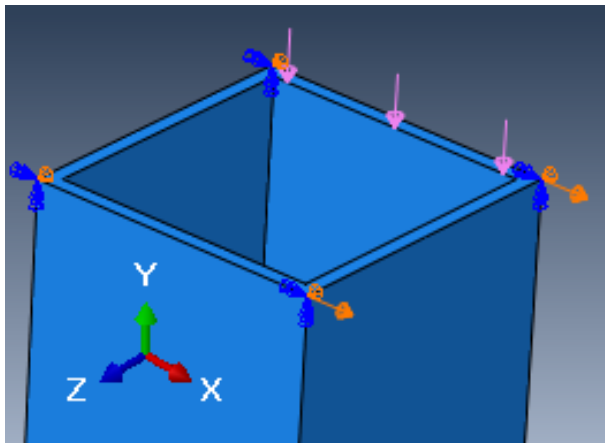


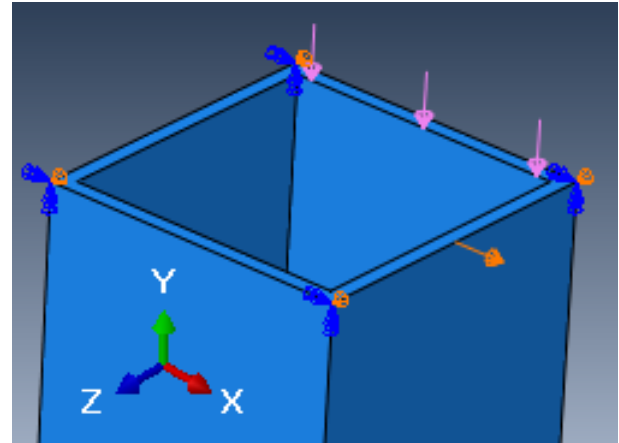
Figure 2: Plastic strain at bottom point of the lower column

## 1.2 Hysteresis Curve of R4W

There has been a mistake that was committed while reporting the hysteresis for the structure. In all the previous simulations, the displacement load was applied at two points but in recent simulation it was applied at only one point to check if it brings any change to the force that is being recorded for plotting the hysteresis curve. The force recorded in recent simulation was double the magnitude of force in previous simulations.



(a) Cyclic Displacement applied at two points



(b) Cyclic Displacement applied only at the mid-point

This blunder has been rectified and simulations were performed to compare Hysteresis for isotropic hardening, Hysteresis for kinematic hardening and experimental hysteresis curve. The graphs below display the comparison.

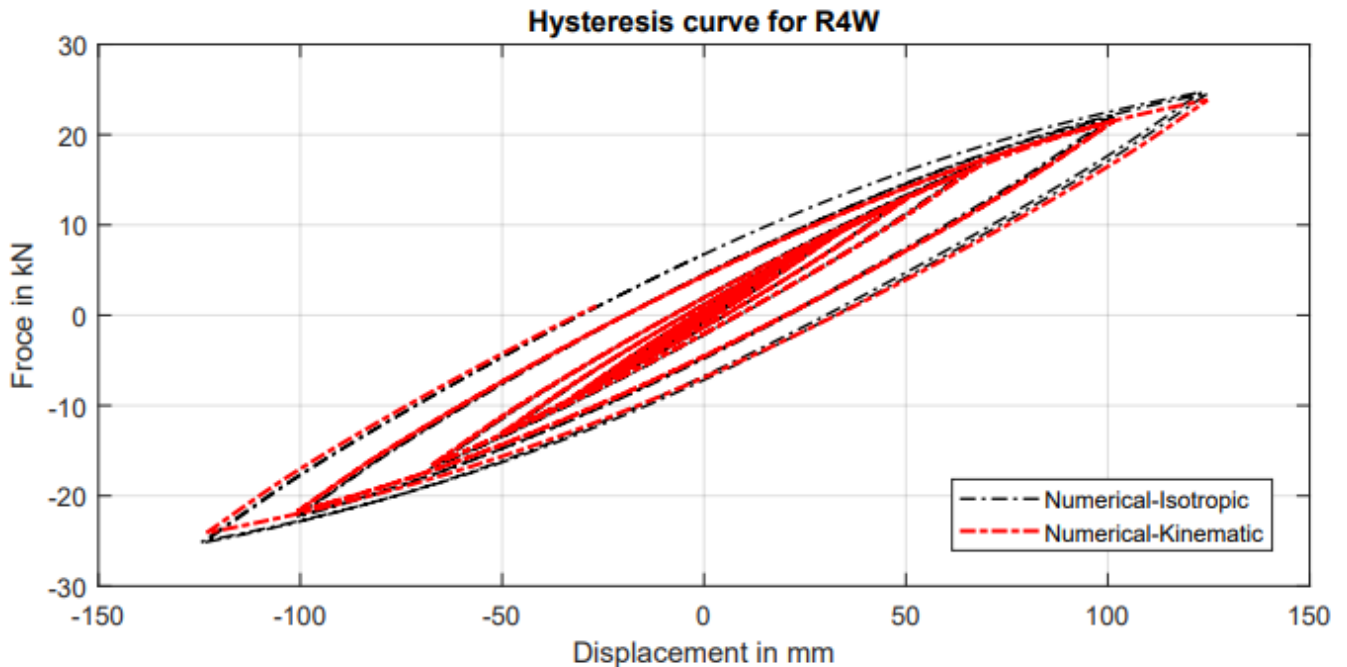


Figure 3: Comparison between Numerical Kinematic Hysteresis and Numerical Isotropic Hysteresis

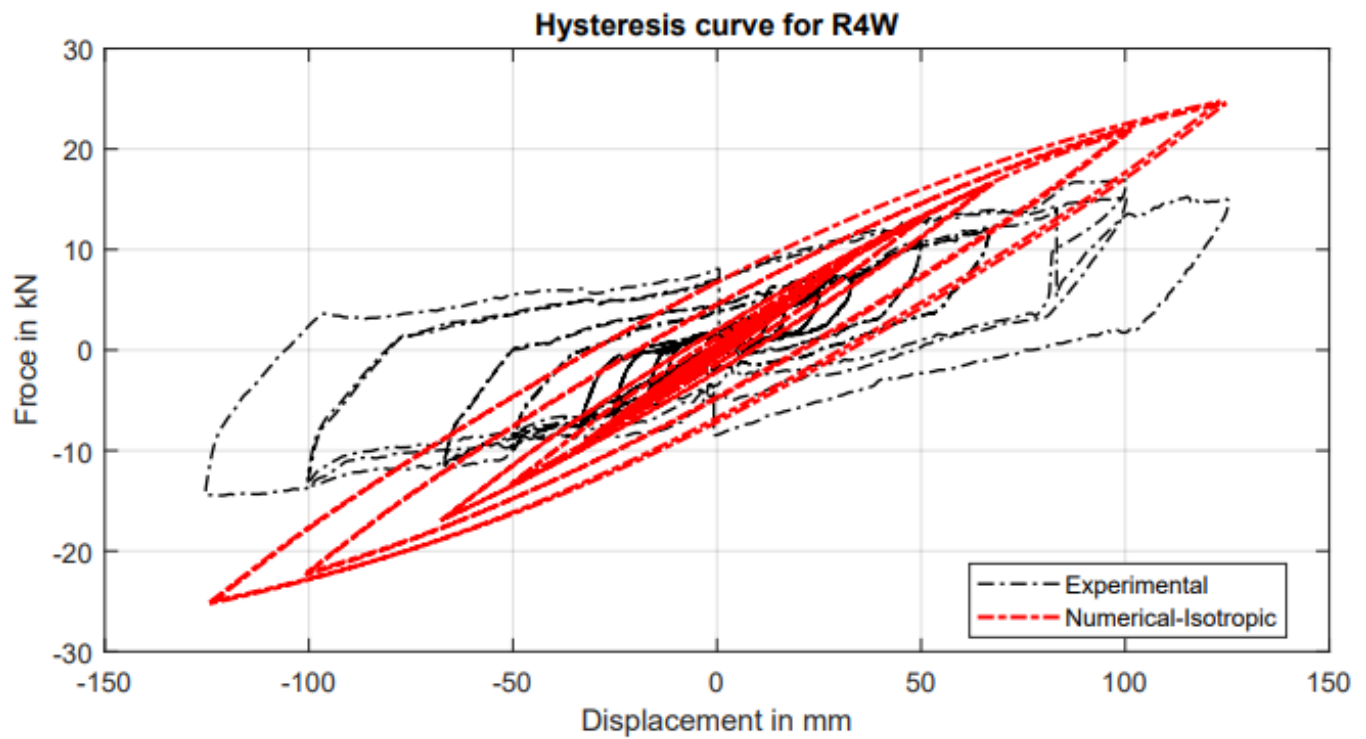


Figure 4: Comparison between Experimental Hysteresis and Numerical Isotropic Hysteresis

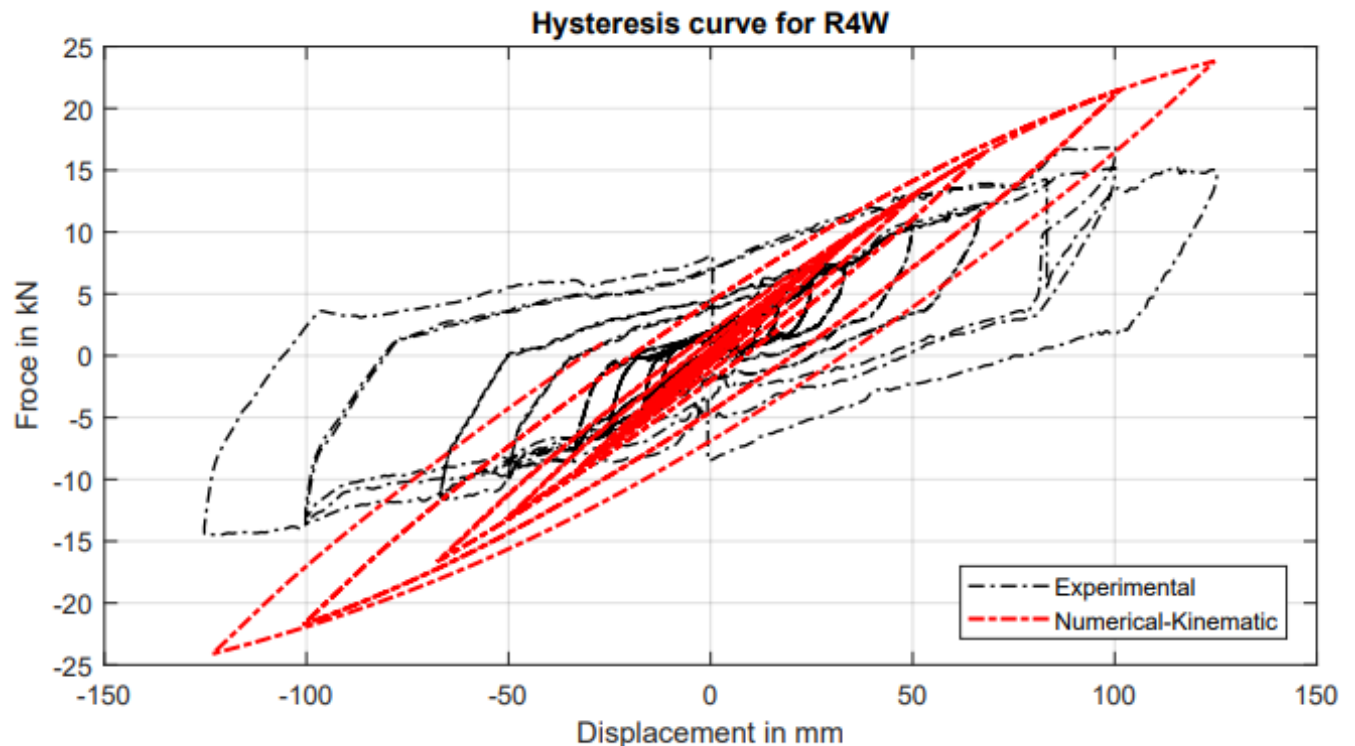


Figure 5: Comparison between Experimental Hysteresis and Numerical Kinematic Hysteresis

# *Seismic Evaluation of R4W*

## *Results from Shell Model*

---

In the previous reports it was seen that the forces corresponding to the applied displacement load were larger in the numerical model as compared to the experiments. This means the model was stiffer than the experimental setup. In order to rectify this problem, a new model was created with shell elements and results obtained were in close proximity with experimental observations and data. In the shell model appropriate thickness was assigned to each structural element. With this, the only difference left between continuum element model and shell model is the presence of weld joint and fillet joints in the beam.

Unlike previous reports, this report mostly constitute the comparison between experimental and numerical results and will not focus much on modelling details. Two simulation were performed, one with spring and another without spring. The hysteresis curve do not match exactly but the skeleton curves obtained from numerical simulation do resemble the experimental one. Along with the detailed comparison between experimental and numerical results, a difference between the results obtained the two simulation are also shown.

## **1 Results from Numerical model**

The results shown in this report are extracted from two FEM models. One model had a spring attached at the end of the beams while the other had no spring. There were differences in results related to forces and especially shape of the hysteresis curve. Out of the two, hysteresis from model with spring was closer to the experimental hysteresis. Since the model with spring is better, the output fields like stress and strain filed are taken from this model and not from the other model. Along with this the report also gives information about the internal energy and dissipation energy in model with spring in the subsection .

### **1.1 Stress field and Plastic Strain field**

In both the model, materials were modelled using bilinear model. Talking about the stress field, it can be seen that is similar to what has been observed in the previous models. The stress field near connection between beam and columns is intense. The values can be seen from the legend shown in the Figure 1.

Discussing about the plastic strain field, it is evident that this filed will be intense in the same region where the stresses were large. The figure 2 displays the contour plot of the plastic strain. The maximum plastic strain was recorded at the corner points of the beam and the strain value was approximately 4.5%. It clearly exceeds the maximum strain recorded in strain gauge number 10 used in the experiment which records a maximum strain of 0.8%. It should be kept in mind that the direction along which the strain is recorded can be different in the two cases but the huge difference in value confirms that failure will occur at these points only.

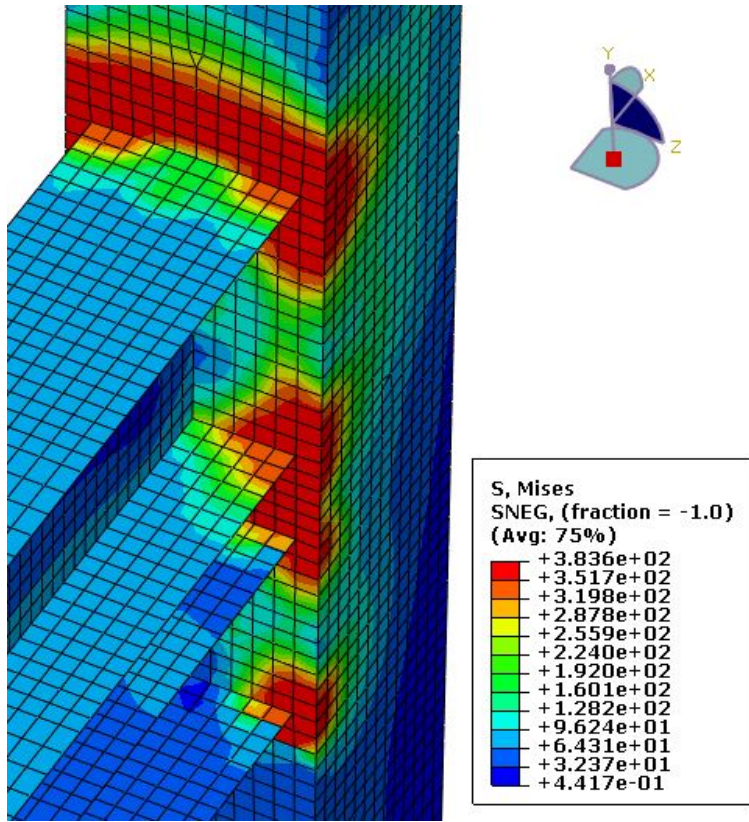


Figure 1: Stress field (von Mises) near beam column connection (Spring was used in this model)

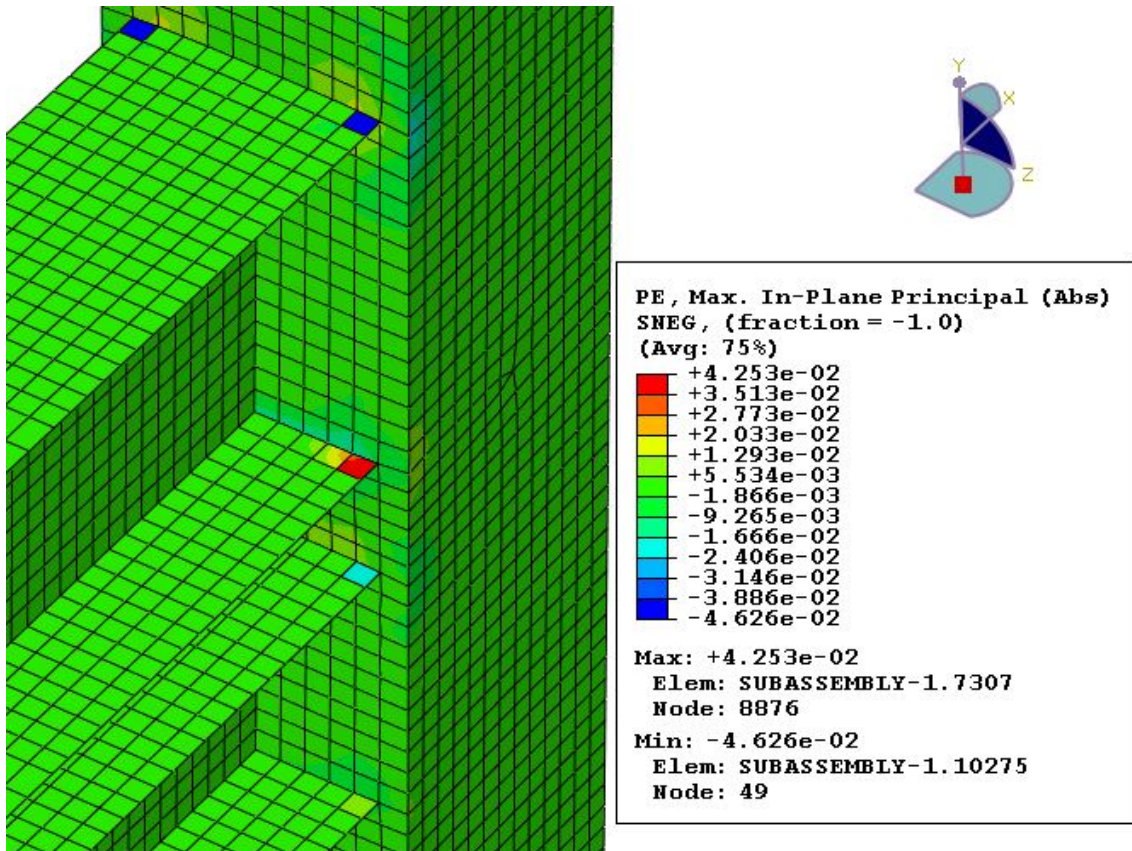


Figure 2: Plastic strain field near beam column connection (Spring was used in this model)

## 1.2 Hysteresis and Skeleton Curve

Figure 3 shown below displays the hysteresis curve obtained for the two numerical models. It should be noted that the use of spring in numerical model has made the shape of the curve a bit similar to the experimental hysteresis.

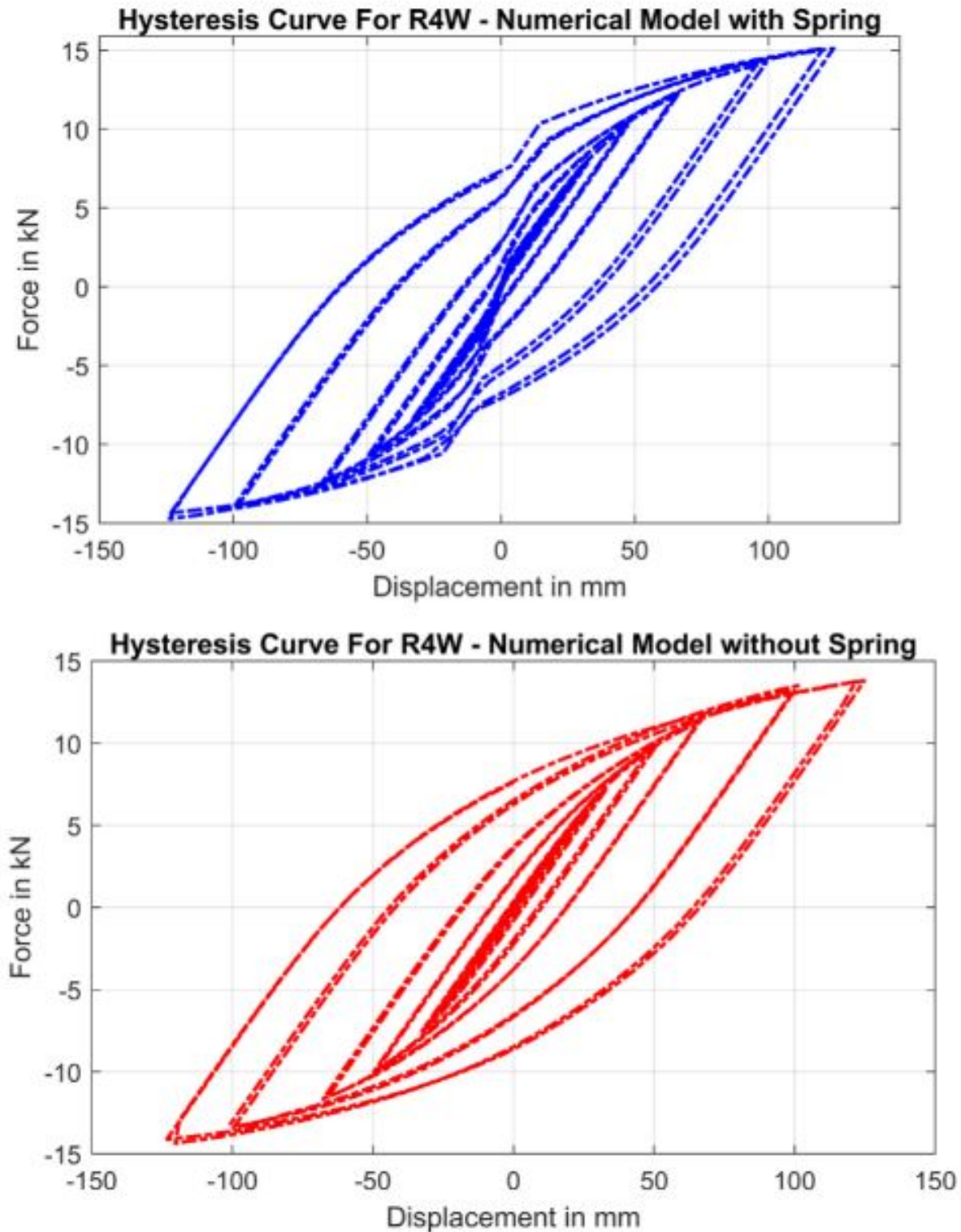


Figure 3: Hysteresis curve from Numerical Model

Now, figure 4 below that compares skeleton curves of the two model and that of the experimental curve. It can be seen that the skeleton curves of both the model very well resemble the experimental skeleton curve. The data for skeleton curve was taken out from the hysteresis data. Because of this exact data is not used to plot this curves.

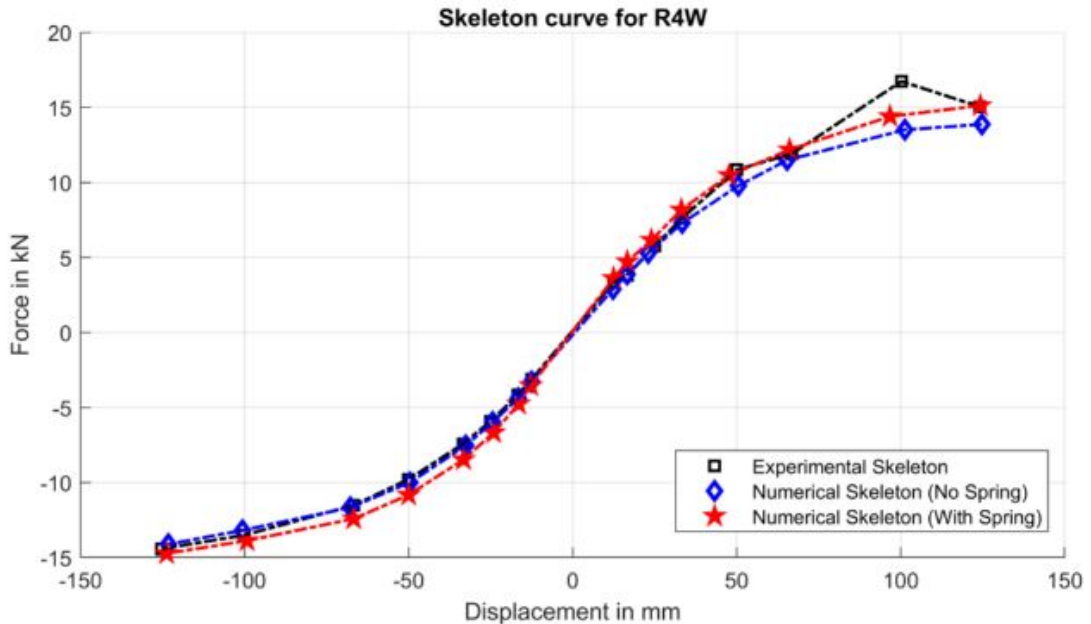


Figure 4: Skeleton curve of R4W

Although figure 4 shows that there are some differences in the skeleton of the model with spring and the experimental skeleton but the experimental hysteresis curve better resembles the hysteresis of spring model than the one without spring. This can be seen from Figure 5 and Figure 6.

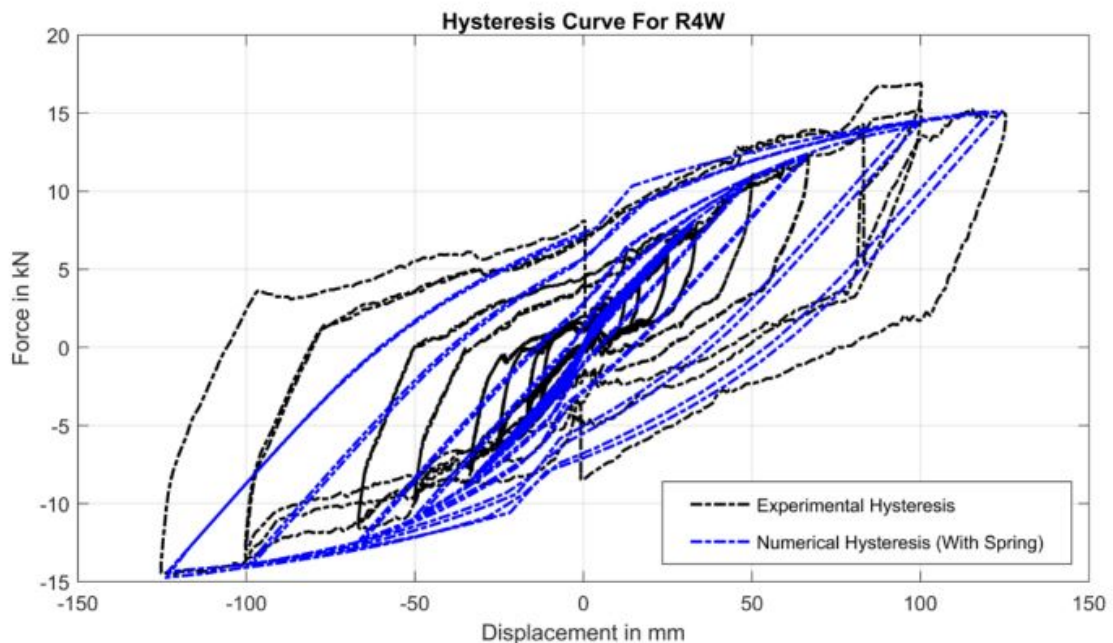


Figure 5: Comparison of Experimental Hysteresis and Numerical Hysteresis (With Spring)

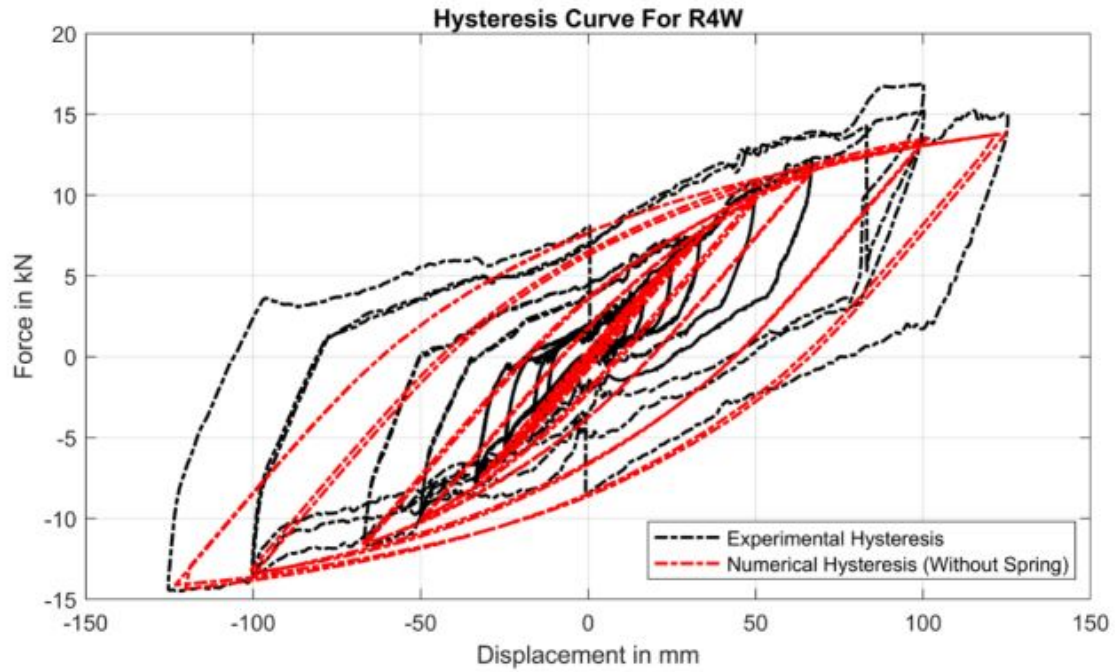


Figure 6: Comparison of Experimental Hysterisis and Numerical Hysterisis (Without Spring)

### 1.3 Internal Energy and Energy Dissipation

From the last subsection it can be observed that the skeleton of numerical and experimental hysteresis do match well but the area under the curve for the two curves is not the same. It can be attributed to the fact that in a experimental setup there is friction and plastic dissipation that are the biggest contributor towards dissipated energy. But in a numerical model the energy is dissipated through only plastic dissipation. This can be seen in Figure 7.

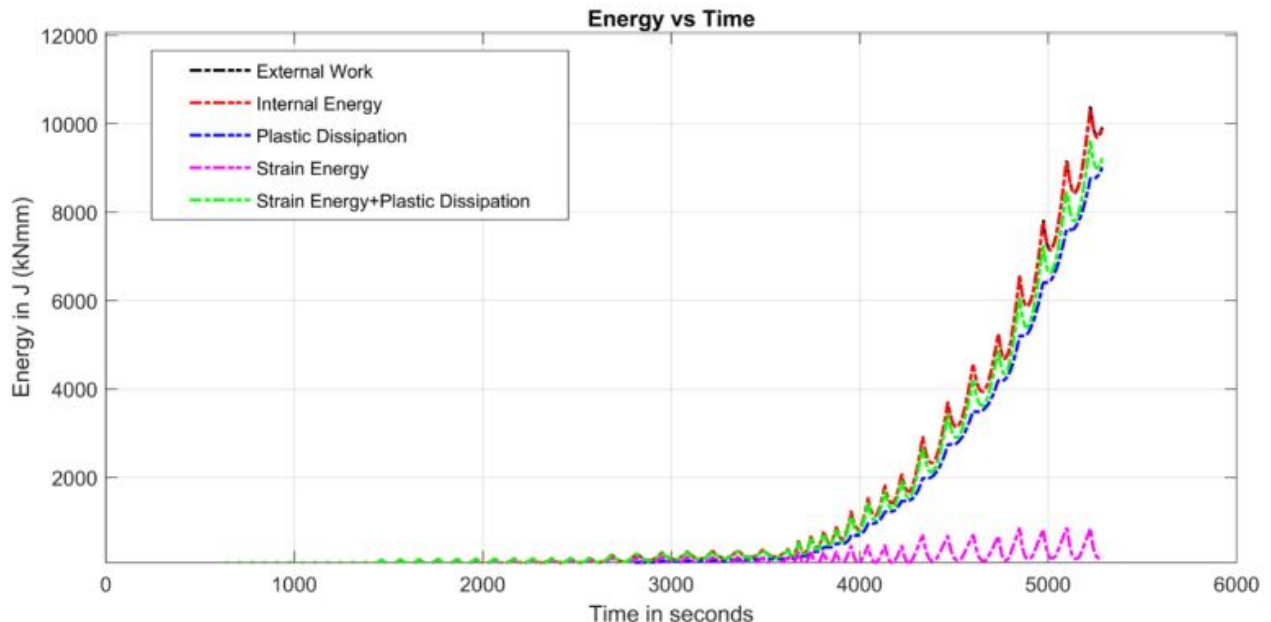


Figure 7: Evolution of energies in Numerical Model (with spring)

The external work (black curve) and internal energy (red curve) have the same value at all points in time. The internal energy is distributed throughout model in two parts - plastic dissipation and strain energy. In Figure 7 it can be seen that the sum of strain energy and plastic dissipation resembles the shape of the internal energy curve but there are still some differences in the values. The possible reason for this could be that the energy stored in the two springs (attached at the end of the two beams) was not taken into consideration.

Also, let's have a look at the cumulative internal energy of the model in Figure 8. One should keep in mind that internal energy for numerical model is equal to the external work since there is no friction. Also, in the research paper cumulative dissipated energy at different drift level is shown but in Figure 8 cumulative internal energy at different drift level is displayed. Both the curves have differences. One has been mentioned and other difference is that the maximum cumulative internal energy recorded is 10kJ at 3.7% drift but in experiment 12kJ of heat was dissipated as we reach 3.7% drift. This means in order to match experimental energy levels we need to model and add some energy dissipation elements to the model.

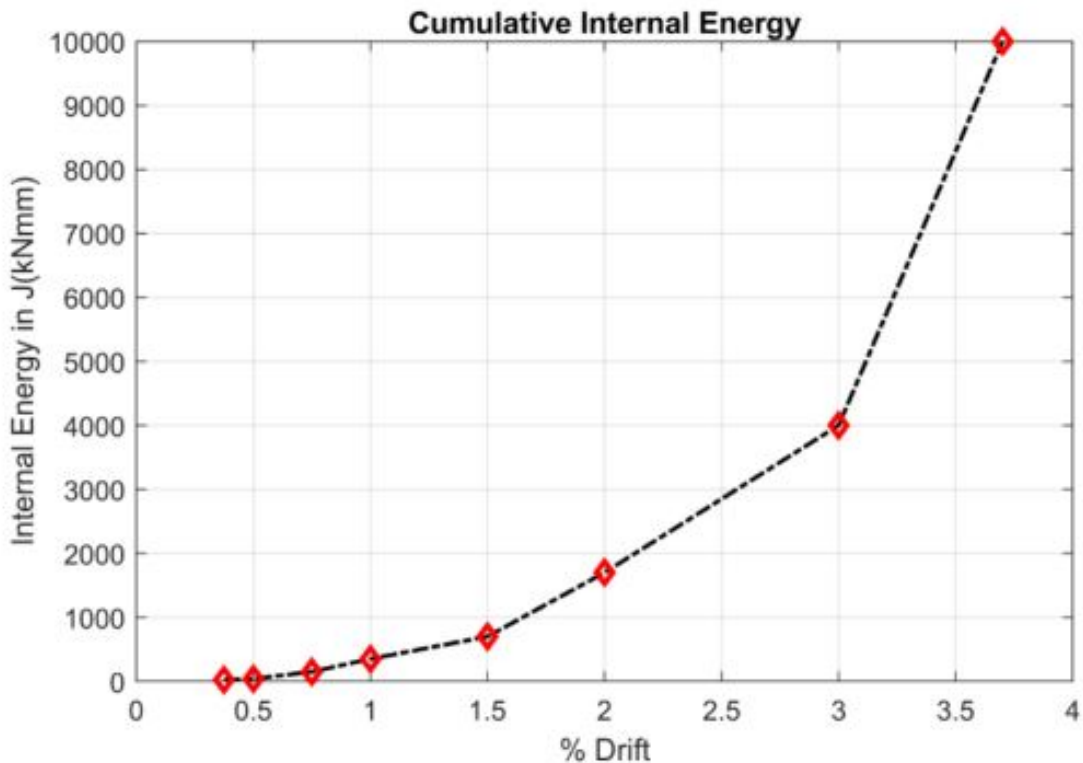


Figure 8: Cumulative Internal Energy of Numerical Model (with spring)

---

# *Seismic Evaluation of R4W*

## *Results from Shell Model with Friction*

$\mathcal{E}$

### *Why solid model has higher stiffness ?*

In the last report results from a model were presented in which the friction force at the end of the beam were modelled using a spring with the following force displacement characteristics.

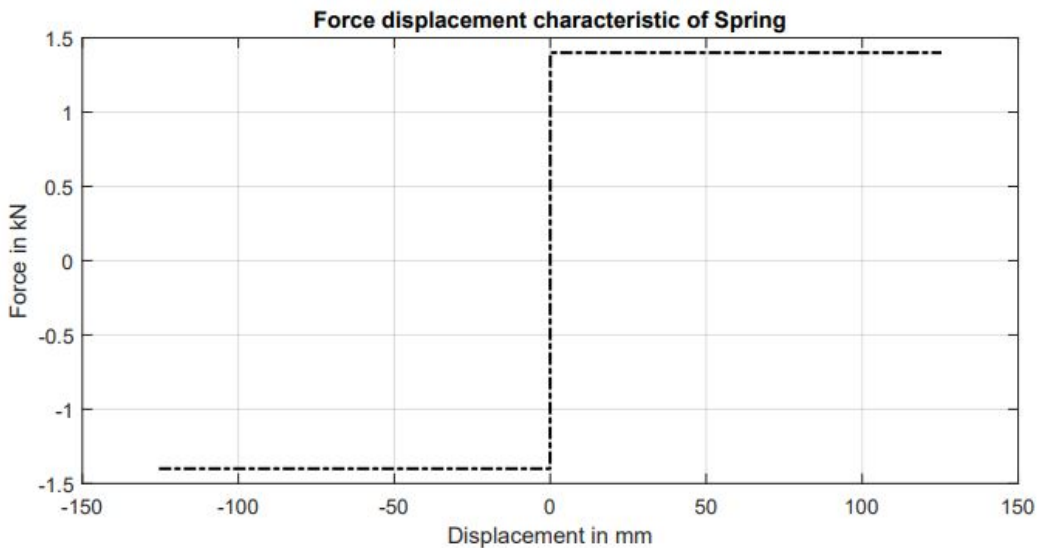


Figure 1: Force vs Displacement for Spring used for friction modelling

It was found that the skeleton curve and hysteresis curve of the model were closer to the experimental one as compared to models that didn't have springs. But if we compare the dissipated energy, then as per the model there was a dissipation of 10kJ and in experiments 12kJ of energy was dissipated. So, to rectify this difference, friction was applied at the end of the beam. The model used to define this friction was

$$\mu = \mu_k + (\mu_s - \mu_k)^{-d_s \gamma}$$

Here,

$\mu_s$  is the static friction coefficient

$\mu_k$  is the kinetic friction coefficient

$d_s$  is the decay exponent

$\gamma$  is the slip rate

In the model,  $\mu_s = \mu_k = 0.5$  and  $d_s = 0$  was used. The magnitude of the contact force was 2800N. From this the maximum friction force value can be found to be equal to 1400N. It was observed that value of energy dissipated recorded from this model was very close to the experimental

value. Although the value of total dissipated energy was matching, the value of dissipated energy was less at smaller drifts as compared to experimental values.

## 1 Results from Shell Model with Friction

The results from this simulation are similar to the results of the previous simulation but are more accurate in terms of energy dissipation because of the friction element incorporated in this model. Like the previous reports; hysteresis curve (Figure 3-4), skeleton curve (Figure 5) and energy curves (Figure 6-8) will be reported as results. Strain field is not shown because it is same as the strain field shown in the previous report. Hardly any difference can be found.

In figure 3, comparison between experimental hysteresis and the hysteresis curve obtained from the numerical model (with friction) is made. It can be seen that the numerical hysteresis covers more area of the graph as compared to previous numerical curves. Also, at lower drifts the behavior is not purely elastic as some nonlinearity and non zero area under curve can be observed. Affect of this will be seen in the cumulative energy dissipation curve shown in Figure 7 where one can see that for drifts in the range 0.375 - 1% significant energy dissipation was observed. In Figure 6, **total energy dissipation is the sum of plastic dissipation and frictional dissipation.**

Let's have a look at these figures.

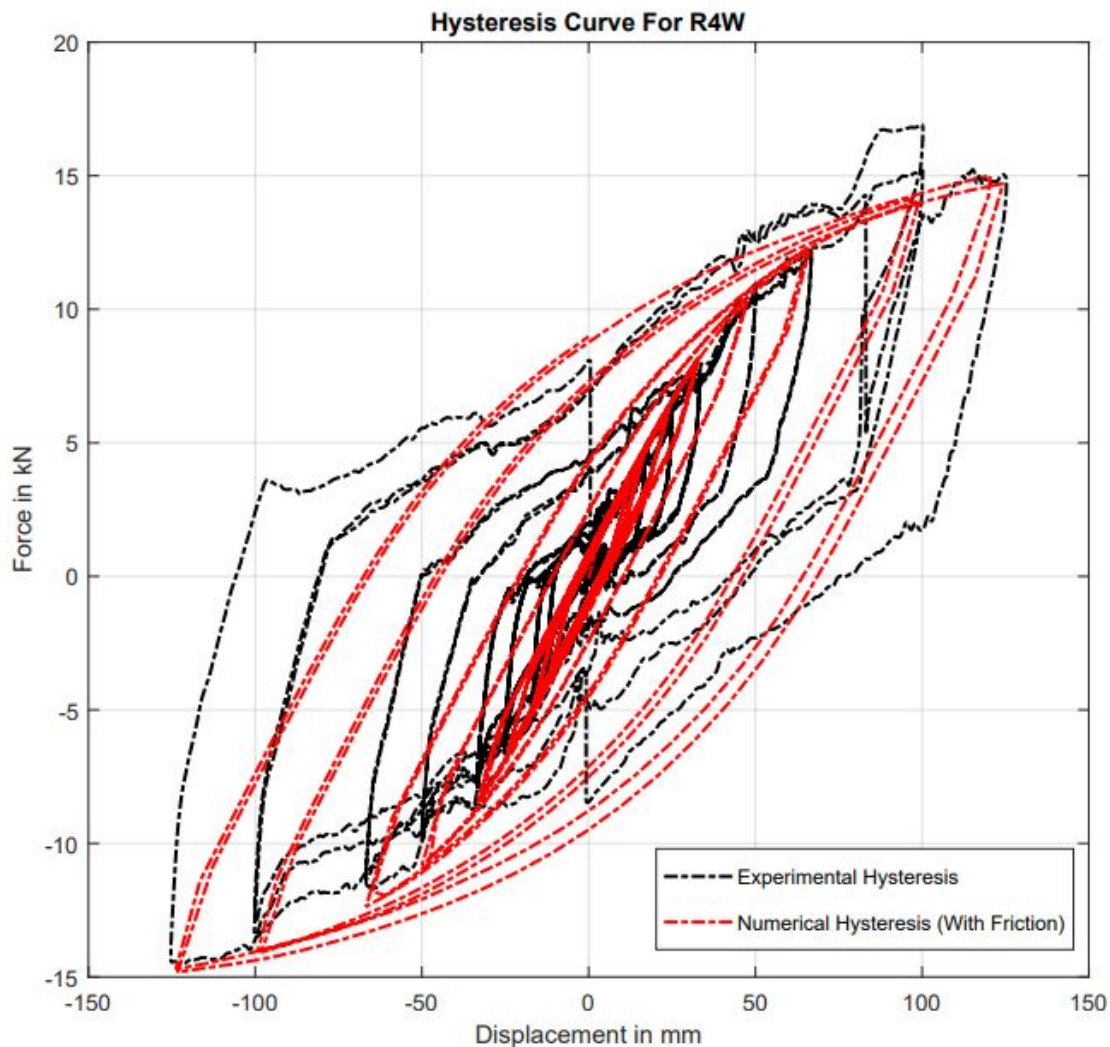


Figure 2: Comparison of Experimental Hysteresis and Numerical Hysteresis (with friction)

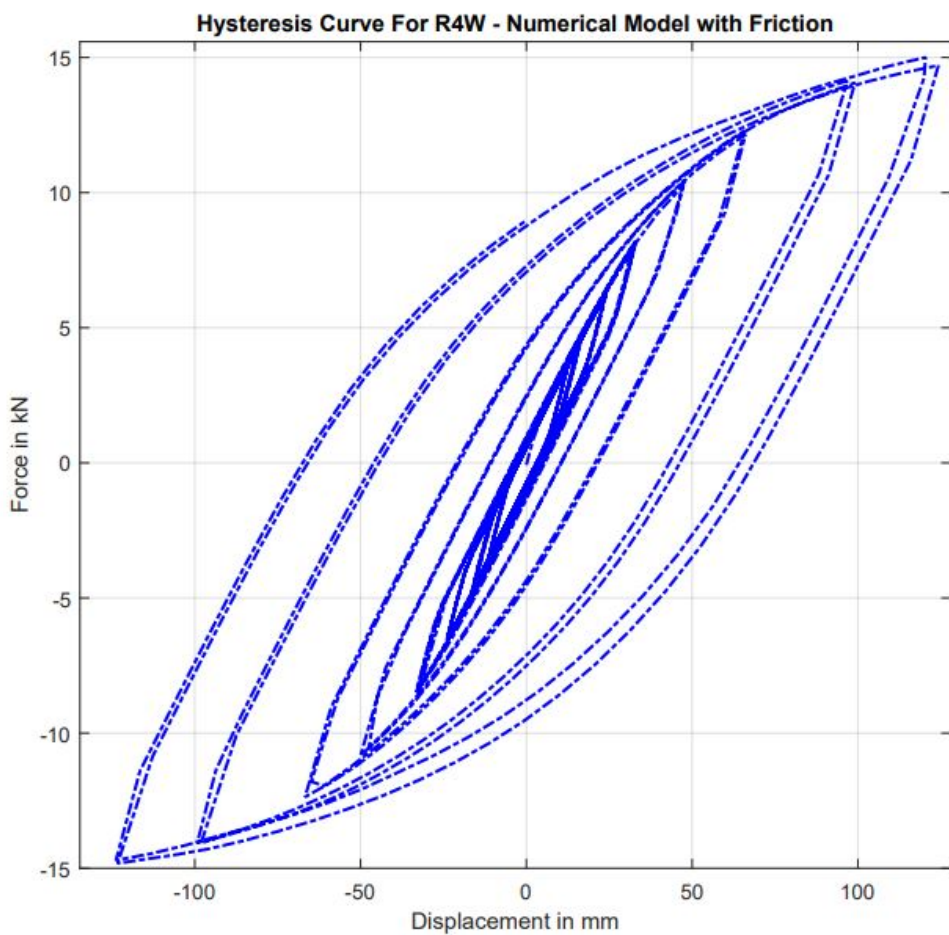


Figure 3: Numerical Hysteresis (Model has friction)

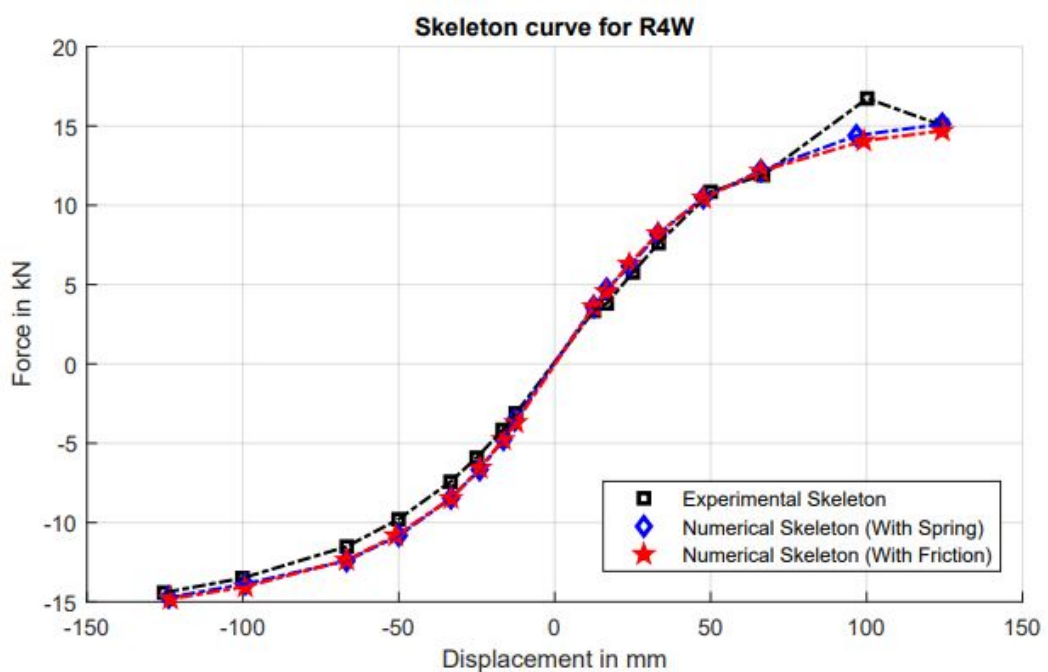


Figure 4: Skeleton curve for R4W

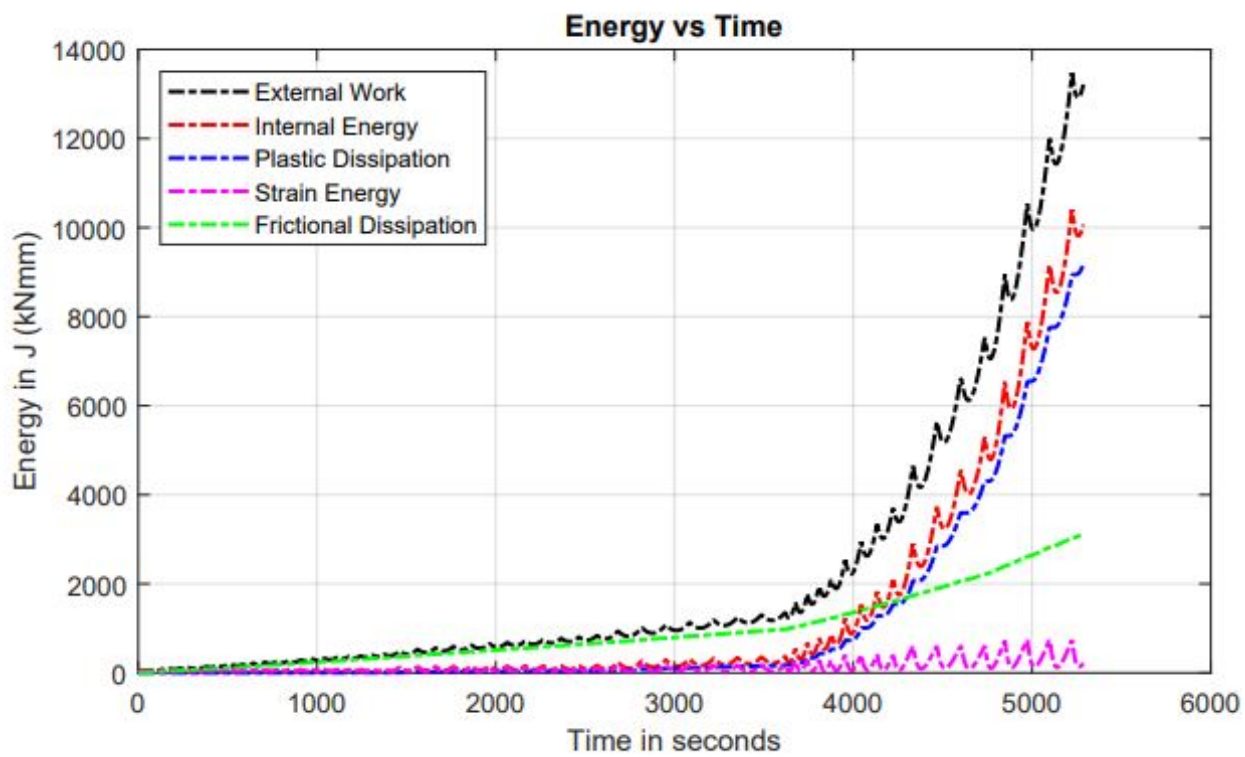


Figure 5: Evolution of Dissipation energy in Numerical Model (with friction)

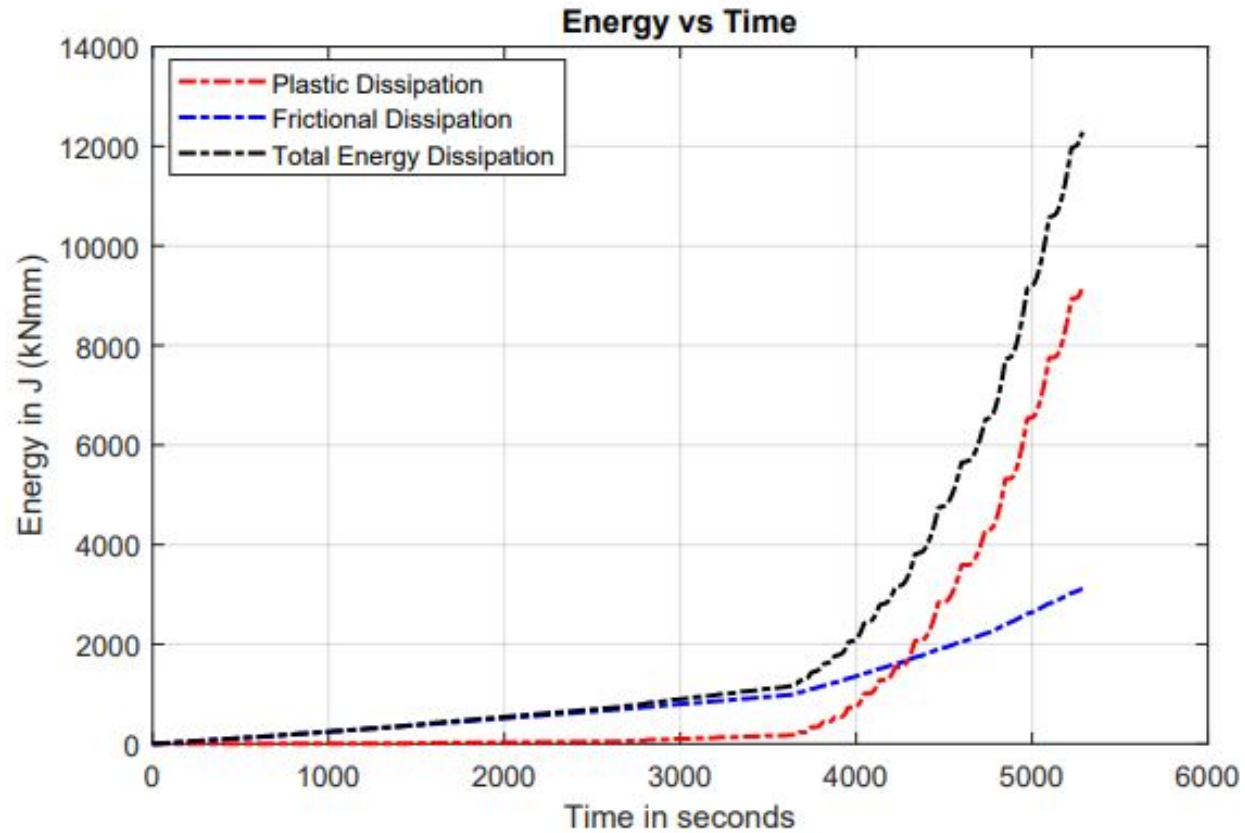


Figure 6: Evolution of energies in Numerical Model (with friction)

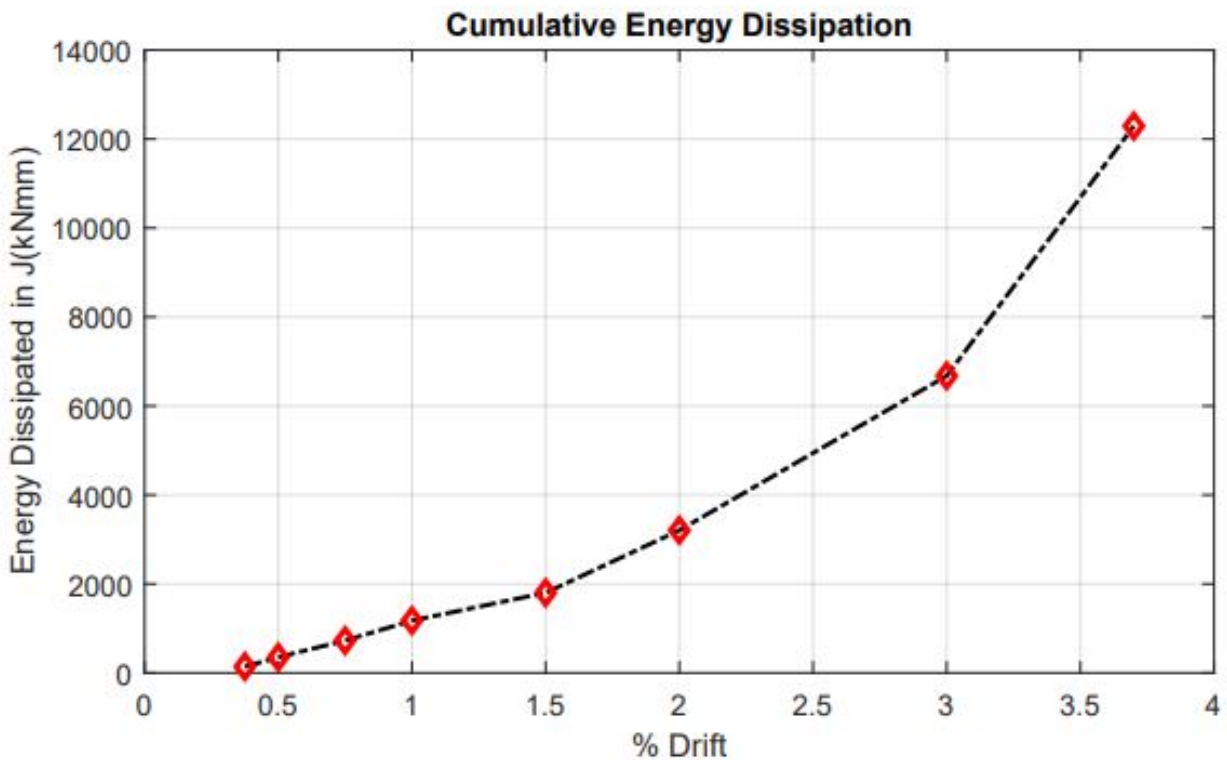


Figure 7: Evolution of energies in Numerical Model (with friction)

## 2 Why model with solid continuum elements has high stiffness than shell element model?

While doing simulations with solid continuum elements it is really important to choose mesh element type keeping in mind the geometry of the problem. This is very general statement but in actual this was the mistake that increased the overall stiffness of the structure.

Let's have a look at some suggestions which a person should keep in mind while modelling structures with thin walls. These suggestions were found in [ABAQUS documentation](#) and through an old discussion on [ResearchGate](#). The possible reason that resulted in increased stiffness of the model were **volumetric locking** and **choosing tetrahedral elements in region of high stress**.

If volumetric locking is suspected, check the pressure stress at the integration points (printed output). **If the pressure values show a checkerboard pattern, changing significantly from one integration point to the next, volumetric locking is occurring.** Choosing a **quilt-style contour plot** in the Visualization module of Abaqus/CAE will show the effect. This phenomenon was checked and was observed in our solid model too. The stress field was not smooth but was more random. While in the shell model, the field was smooth. A comparison between shell model and solid model has been shown in figure 8 and figure 9 where the stress field of both the models can be observed. In addition to this **shear locking** can also be observed when the element length is equal to the wall thickness. This can be seen in our model in Figure 10.

In report 2, a picture of the meshing in the model is shown. It can be seen that the region of connection between beam and column was meshed with tetrahedral elements and the rest of the region with brick elements. As a rule, these elements should not be used except as filler elements in noncritical areas. As per the ABAQUS documentation, first-order triangles and tetrahedra are

usually overly stiff, and extremely fine meshes are required to obtain accurate results. This fact was also a contributor to extra stiffness of our model. Also, if we have a look at the dimension of column we can see that the ratio of cross sectional length and wall thickness is approximately 20. If this much difference is observed in dimensions of a problem, then it is better to use shell elements.

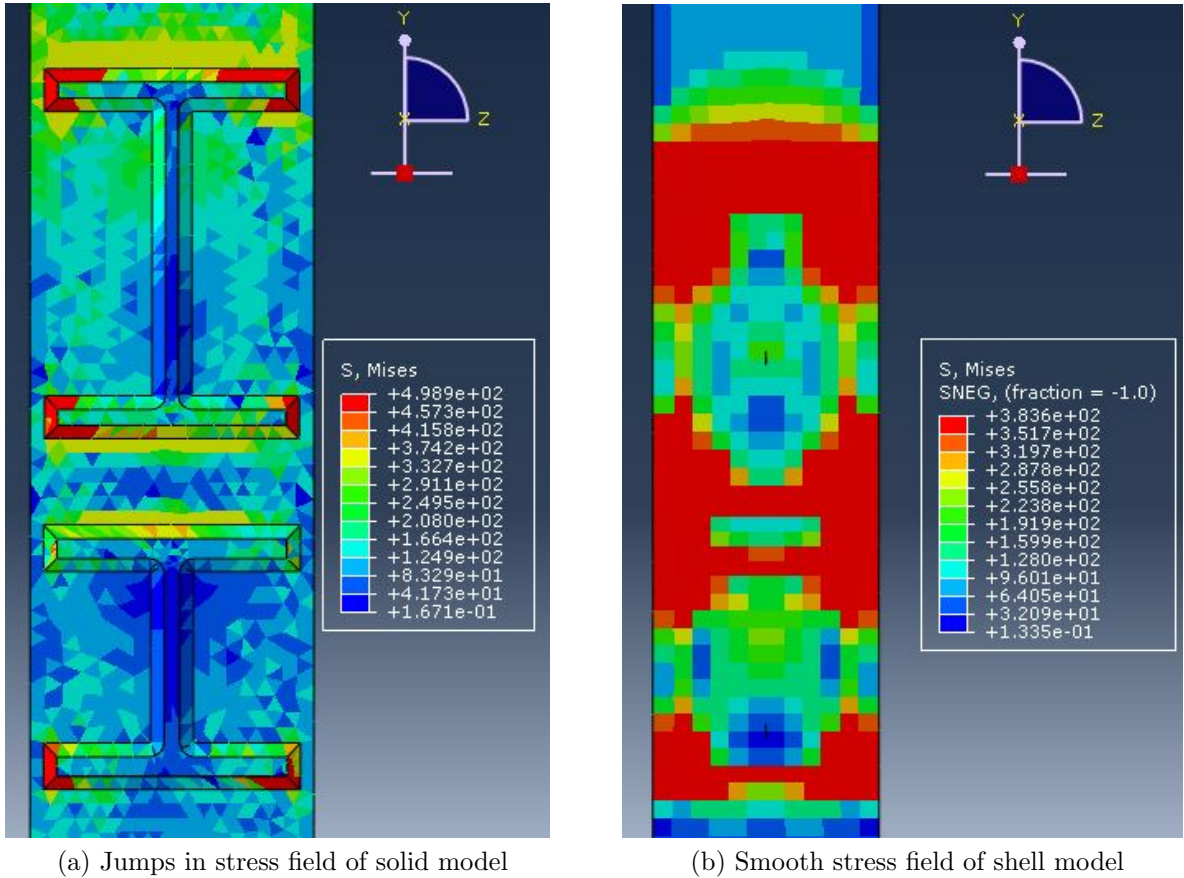


Figure 8: Stress field comparison between solid model and shell model

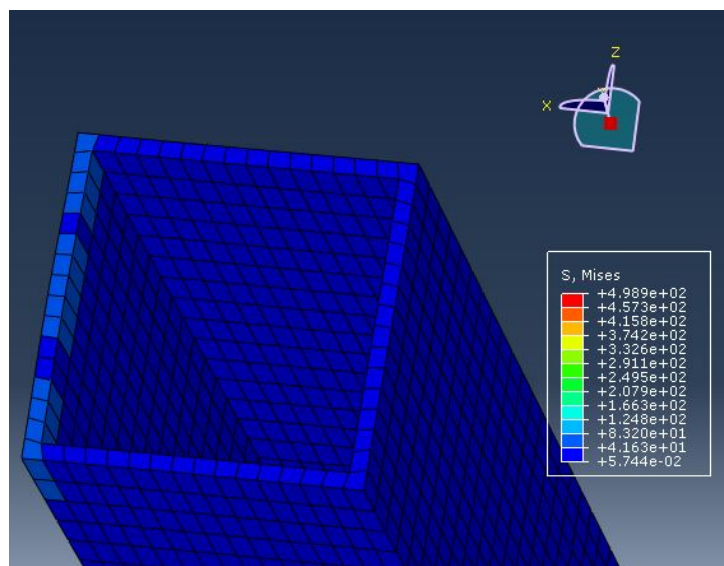


Figure 9: Wall thickness = element thickness >>> Shear locking

# Contact Analysis

Modelling contact using finite element models is quite an involving task as the results depends on a number of factors. These factors include selection of master and slave surface, using an appropriate discretization method and proper meshing of master and slave surface. Application of suitable interaction between master and slave surface is also necessary to get desire results. The report gives an account on the effects of these parameters on the results of a simple contact analysis. Theoretical and experimental results will be compared to observe the effects of these parameters.

## 1 Problem on Contact Analysis and Theoretical Results

Here, we will consider a simple problem in which a block slides over a floor having a friction coefficient of  $\mu = 1$ . Other details related to this problem are:

Dimension of Block :  $10 \times 10 \times 10$

Thickness of the faces of the block : 5

The block is modelled using shell elements. It was constructed by extruding a cross-section of  $10 \times 10$  to height of 10. Due to this method the block will have an open face at top and at bottom. A plate of same cross section was used to close the top face and the bottom face was kept open. The reason for keeping the bottom face open is to establish similarity with one of the contacts in B1PT0. This contact is similar to the contact between mid plate and the column as in this the edges of the column are in contact with the upper surface of the mid plate.

The floor is a  $100 \times 100 \times 5$  object made up of solid elements. The global coordinate frame is located at one of the corners of this object and the block is placed such that one of the vertices of the open bottom face coincides with the origin and the rest of the vertices lie on the floor. The pictorial representation of the problem can be seen in the figure below:

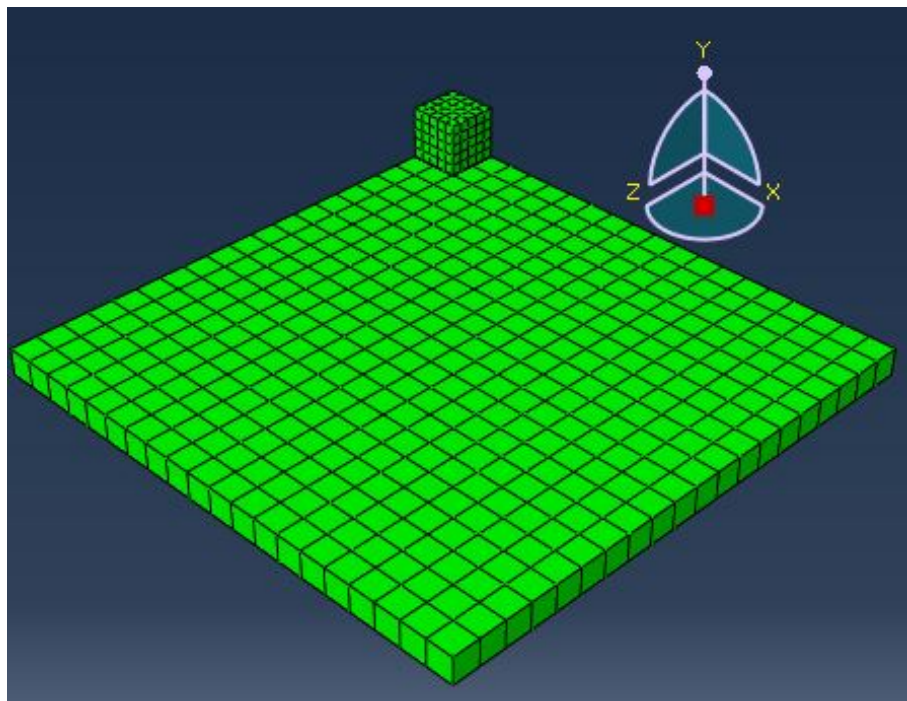


Figure 1: Contact Analysis Problem

The physical quantity that we will be analysing is the frictional dissipation in the process of displacing the block along the diagonal of the floor by a distance of  $20\sqrt{2}$ . During this process a normal force at the top face of the box is applied.

$$F_{applied} = 50t, t \in [0, 1]$$

Hence, the frictional and normal force acting on the box are:

$$N_{box} = 50t$$

$$F_{friction \text{ on } box} = \mu \times N = 50t$$

Calculating the frictional dissipation:

$$E_{frictional \text{ dissipation}} = \int_0^1 F_{friction} ds = \int_0^1 50t \times 20\sqrt{2} dt = 707.1$$

Here,

$$s = 20\sqrt{2}t$$

## 2 Solving the problem in ABAQUS

Six simulation were performed to study effects of aforementioned parameters. Unit system used is : mm, tonne, MPa, N, seconds. Information about some parameters were found using online ABAQUS tutorials. Each simulation was completed in two steps namely Make Contact and Apply Load. In all the six simulation **Surface to Surface** discretization method is used and **Floor** was chosen as the **Master surface** and the **four edges of the block** as the **Slave surface**. Details and results of the six simulation are discussed below.

### Simulation 1:

Mesh size and mesh type

Block : 2, Quadrilateral element

Floor : 1, Solid Brick element

Contact type : Friction

Friction type : Penalty with  $\mu = 1$

No normal contact interaction was used but to avoid impractical penetrations of one surface into another face to face constraints were used

Time period of Analysis : 1 sec

In the figure below one can observe that only the edges of the block are in contact with the surface.

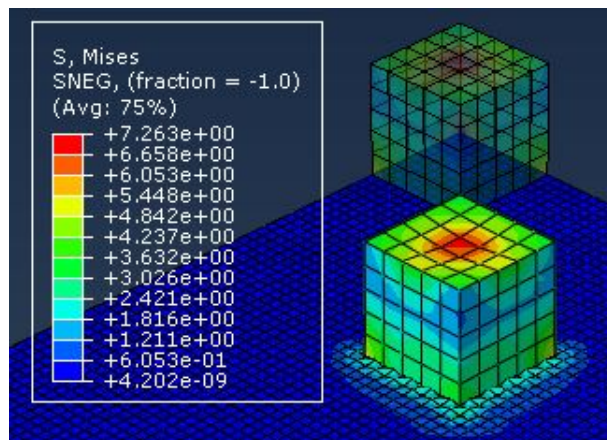


Figure 2: Von Mises Stress in Simulation 1

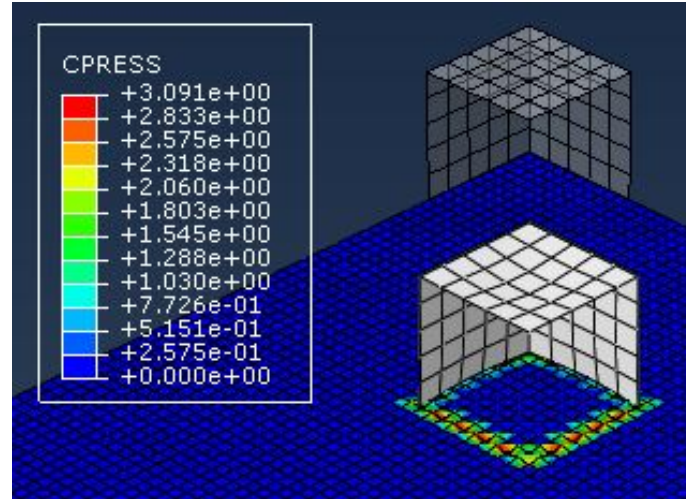


Figure 3: Contact Stress in Simulation 1

### Simulation 2:

Mesh size and mesh type

Block : 2, Quadrilateral element

Floor : 1, Solid Tetrahedral element

Contact type : Friction

Friction type : Penalty with  $\mu = 1$

No normal contact interaction was used but to avoid impractical penetrations of one surface into another face to face constraints were used

Time period of Analysis : 1 sec

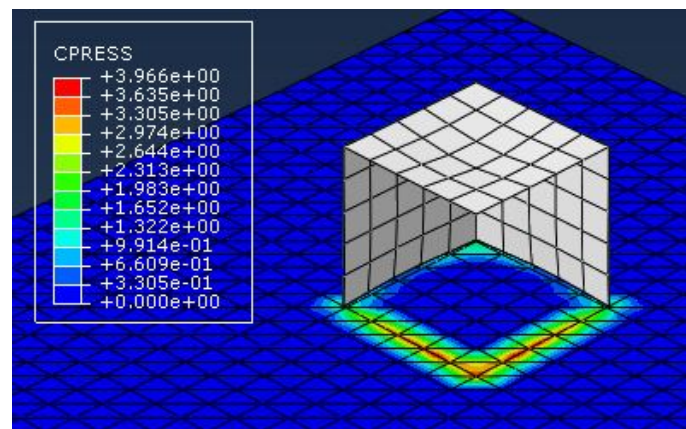


Figure 4: Contact Pressure in Simulation 2

### Simulation 3:

Mesh size and mesh type

Block : 2, Quadrilateral element

Floor : 2, Solid Brick element

Contact type : Friction

Friction type : Penalty with  $\mu = 1$

No normal contact interaction was used but to avoid impractical penetrations of one surface into another face to face constraints were used

Time period of Analysis : 1 sec

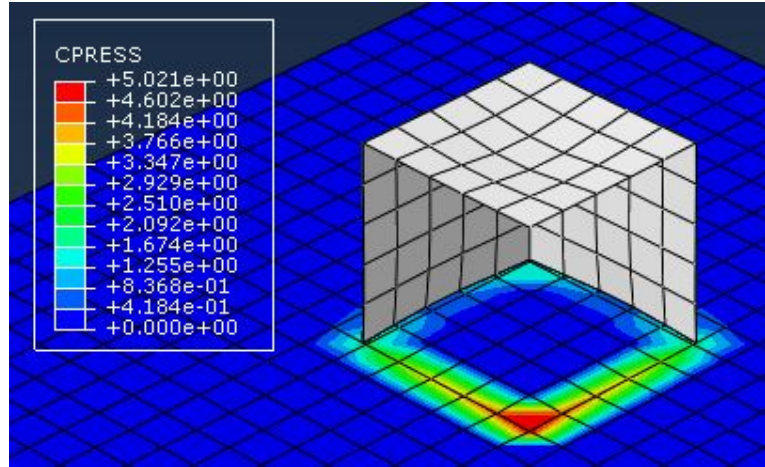


Figure 5: Contact Pressure in Simulation 3

#### Simulation 4:

Mesh size and mesh type

Block : 2, Quadrilateral element

Floor : 3, Solid Brick element

Contact type : Friction

Friction type : Penalty with  $\mu = 1$

No normal contact interaction was used but to avoid impractical penetrations of one surface into another face to face constraints were used

Time period of Analysis : 1 sec

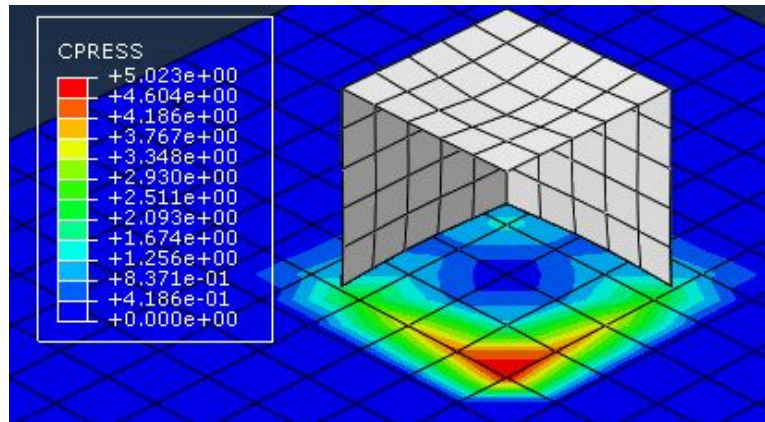


Figure 6: Contact Pressure in Simulation 4

#### Simulation 5:

Mesh size and mesh type

Block : 2, Quadrilateral element

Floor : 5, Solid Brick element

Contact type : Friction

Friction type : Penalty with  $\mu = 1$

No normal contact interaction was used but to avoid impractical penetrations of one surface into another face to face constraints were used

Time period of Analysis : 1 sec

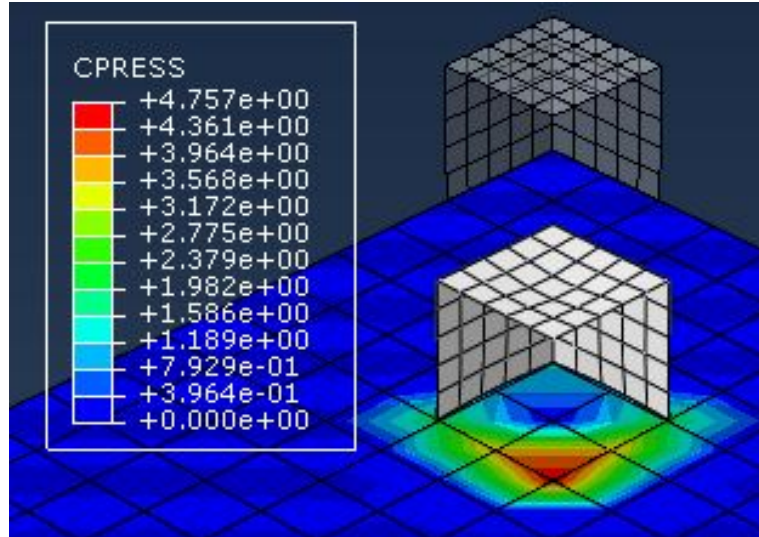


Figure 7: Contact Pressure in Simulation 5

### Simulation 6:

Mesh size and mesh type

Block : 2, Quadrilateral element

Floor : 5, Solid Brick element

Contact type : Friction

Friction type : Penalty with  $\mu = 1$

Normal Contact : Linear, Stiffness = 2000

Also the contact step was propagated in the loading step. In this step the block was forcefully penetrated into the floor by 0.2. This resulted in a additional normal force of 400.

Time period of Analysis : 1 sec

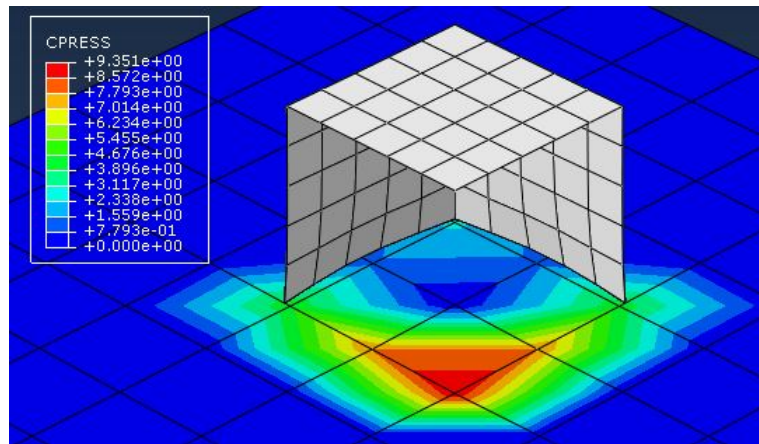


Figure 8: Contact Pressure in Simulation 6

Now, let us look at the cumulative frictional dissipation for each simulation. Figure 9 shows comparison between the first 5 simulation as they have the frictional dissipation in the same range. While, Figure 10 shows the frictional dissipation for Simulation 6 as the energy dissipated in this simulation was more due to the presence of extra normal force.

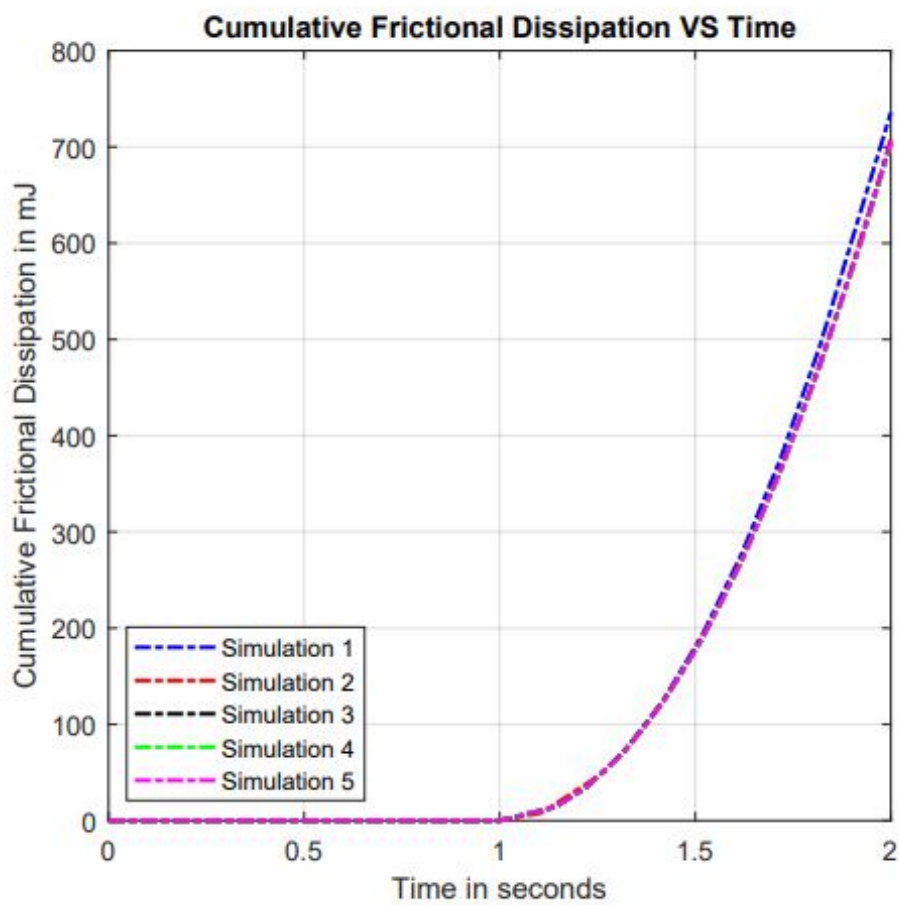


Figure 9: Comparing the frictional dissipation, Simulation 1-5

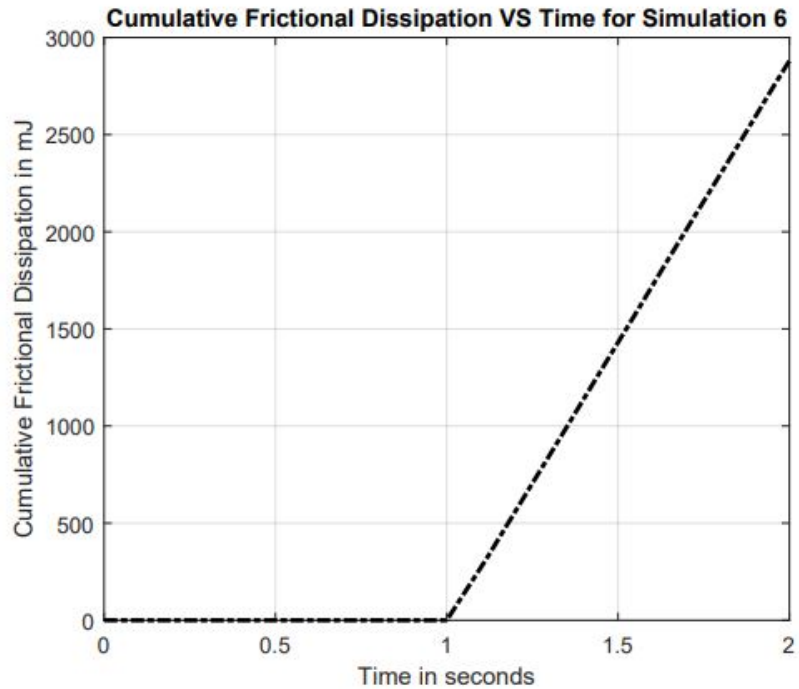


Figure 10: Simulation 6, Frictional Dissipation

Error in Numerical Results of first 5 simulations wrt Theoretical Result		
Simulation	Numerical Frictional Dissipation Value (mJ)	% Error
1	735.57	4.03
2	708.12	0.144
3	704.08	0.427
4	702.13	0.703
5	705.3	0.25

Simulation 6 was performed to know what happens if we activate the Contact Analysis step in the last step i.e. Apply Load. Here, the contact step was created to establish contact between the surfaces before actual analysis starts. Propagating this step to the last step will impose the outputs of this step in the later step. In our case, this output was the normal force arising in the Make Contact step due to the vertical displacement of block by 0.25 into the floor in order to establish contact. Hence, this additional normal force contributed to the frictional force in the Apply load step and therefore increased the cumulative frictional dissipation to 2879.91 mJ.

### 3 Inference from above analysis and Comments about other parameters

#### 3.1 Effects of Mesh Size

From the above analysis it can be observed that meshing Master surface with a coarser mesh as compared to Slave surface provides better results both in terms of output and computational cost. Hence, the surface we select as Slave surface should be more finely meshed. Additionally, if the mesh densities for both the surfaces are same then the Slave surface should be the one with softer material i.e. low density.

#### 3.2 Contact Discretization and selection of Master and Slave surfaces

There are two types of contact discretization in ABAQUS:

1. Node-to-Surface
2. Surface-to-Surface

In **Node-to-Surface** discretization, nodes on one surface, the Slave surface, contact the discretized segments on the master surface. It is not possible for Slave to penetrate the Master surface. It is not possible for the Slave to penetrate the Master surface. Although the nodes of the Master may penetrate into the Slave surface.

**Surface-to-Surface** strategy considers the shape of both the Master and the Slave surface in the region of contact. It enforces the contact condition in an average sense over regions near the Slave nodes rather than on individual slave nodes alone. Large penetration of Master nodes into the Slave surface do not occur with this discretization.

Because of the above reason selection of Master and Slave surface does not matter in case of Surface-to-Surface while above mentioned guidelines should be considered in case of Node-to-Surface discretization.

### 3.3 Tangential Behaviour

ABAQUS offers a number of options to model the tangential behaviour between two surfaces in contact. Let's have a look at these options:

#### Frictionless

With this option there will be no friction between the concerned surfaces and only normal forces will exist.

#### Penalty

This friction formulation allows a small elastic slip even then the two surface should be sticking. ABAQUS will automatically choose the penalty stiffness such that this allowable elastic slip is a very small fraction of the characteristic element length. This slip value is by default  $0.005 \times \text{Characteristic Element Size}$ .

#### Lagrange Multiplier

To model ideal frictional behaviour, Lagrange Multiplier can be used. In this formulation, slipping will not occur until the shear stress between the surfaces cross the critical shear stress.

#### Rough

This formulation specifies an infinite coefficient of friction between the surfaces. This ensures no slipping between the surfaces no matter how high the shear stress.

#### Static-Kinetic Exponential Decay

The mathematical representation of this friction formulation is:

$$\mu = \mu_k + (\mu_s - \mu_k)^{-d_s \gamma}$$

Here,

$\mu_s$  is the static friction coefficient

$\mu_k$  is the kinetic friction coefficient

$d_s$  is the decay exponent

$\gamma$  is the slip rate

### 3.4 Normal Behaviour

Most common normal behaviour used to model normal contact between surfaces are:

#### Hard Contact

This formulation considers that when surfaces are in contact, any contact pressure can be transmitted between them. The surfaces separate if the contact pressure reduces to zero. Separated surfaces come into contact when the clearance between them reduces to zero.

#### Linear

This formulation considers a linear graph between Contact force and overclosure. The user is requested to provide the value of contact stiffness i.e. the slope of the curve.

#### Exponential

In an exponential contact pressure-overclosure relationship the surfaces begin to transmit contact pressure once the clearance between them, measured in the contact (normal) direction, reduces to  $c_0$ .

The contact pressure transmitted between the surfaces then increases exponentially as the clearance continues to diminish.

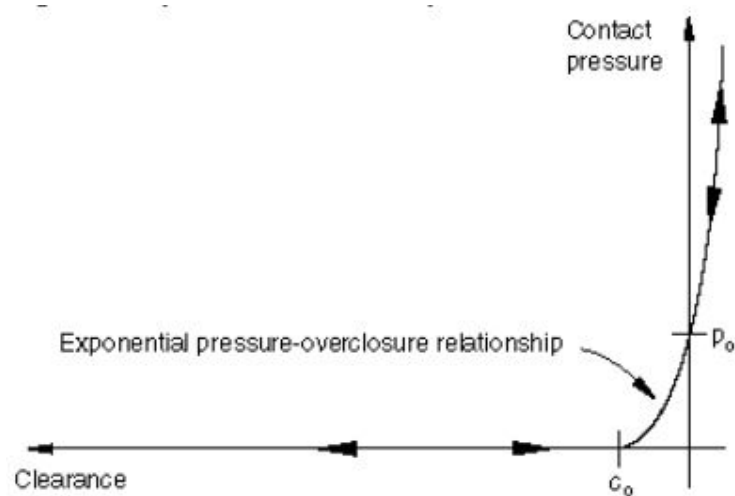


Figure 11: Exponential Normal Contact Formulation

---

# *Seismic Evaluation of B1PT0*

This note presents the results from the numerical analysis of B1PT0 under seismic load. Along with the necessary outputs of the analysis i.e. energy dissipation and hysteresis curve, important details related to modelling this structure are also reported. Unlike R4W, this model consists of unconnected regions due to which it becomes mandatory to model contact between those unconnected regions. Detailed information about contact modelling in B1PT0 will be provided in Section II. Before this, some features of B1PT0 related to parts and their materials will be reported in Section I. In Section III, the most important aspect of this simulation i.e. fracture modelling will be discussed. Section IV will deal with the planning of simulation into steps of appropriate time period. The last section i.e. section V will display the results obtained from multiple simulation of B1PT0.

## 1 Basic Details about Finite Element Model of B1PT0

The model of B1PT0 is more complex as compared to R4W where all the elements were connected to each other. In B1PT0, all the structural elements are modelled using shell elements and there are 4 unconnected regions: Upper Module, Lower Module, Box and the Rod. Each module contains a column, beam and a plate at the end of column. In order to transfer loads from the top module to the bottom module we need to define contact between these four elements of the structure. The rod will be connected to the mid point of bottom and top plate using **surface to node tie constraint**. The details of contact established between the rest of the elements will be discussed in the subsequent section. The dimension of beams and columns used in this model were similar to those used in R4W. The cross section of the box used in this simulation is 127 mm×127 mm and the height is 379 mm. The cross section of the Middle plate used in this simulation is 139 mm×139 mm and there is a square hole in the middle whose . The reason for choosing this increased cross section for Middle plate is to avoid distorted and small elements at the edges of the plate after the plate is merged with the box. This prevents unnecessary mesh transitions in the model that can cause convergence and accuracy issues.

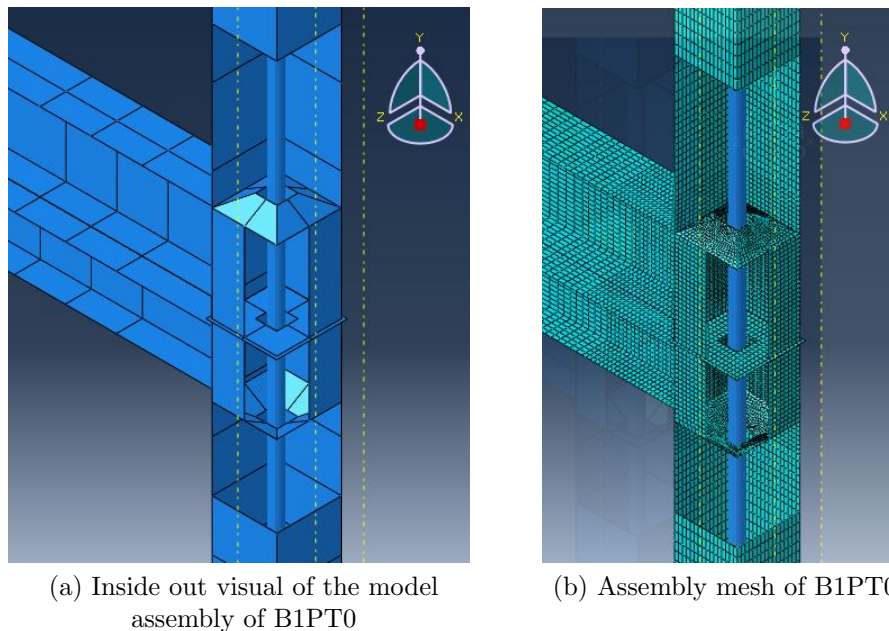


Figure 1 displays the in and out details of the B1PT0 model. It should be noted that the Rod was modelled using **beam elements** and in the figure the profile of the beam has been rendered to get better visual of the model. Figure 2 shows the meshing of the assembly. The meshing has been done keeping in mind the contact pairs i.e. master and slave surface. An account on meshing of contact pairs has been given in Report 6 on **Contact Analysis**. This is necessary to attain good accuracy in terms of contact based outputs.

## 2 Contact modelling in B1PT0

As it has been mentioned in the previous section that there were 4 unconnected regions in the model. One connection was built using **surface to node tie constraints** between the top plate and uppermost node of the rod and similarly between bottom plate and lowermost node of the rod.

Apart from this, there are four contact pairs in the assembly. These are:

1. Outer surface of Box and Inner surface of Upper column - Surface to surface contact
2. Outer surface of box and Inner surface of Lower Column - Surface to surface contact
3. Upper surface of Middle plate and the nodes at the lower end of the Upper Module - Node to Surface contact
4. Lower surface of Middle plate and the nodes at the upper end of the Lower Module - Node to Surface contact

For all the contact pairs **surface to surface discretization method** is used. For all the contact pairs **Small sliding** has been applied which unlike **Finite sliding** commands the ABAQUS to establish the relationship between the slave nodes and the master surface at the beginning of the simulation which significantly reduces the computation time. Another reason for using **Small Sliding** is that it allows the user to pass a numerical clearance to the solver irrespective of the physical dimension of the clearance in the model. This feature has been used in this model also where a clearance of 0.1 mm has been provided in the third and the fourth contact pair. It is shown in figure 3. For fast convergence of the solution **zero** clearance was passed for these two contact pairs.

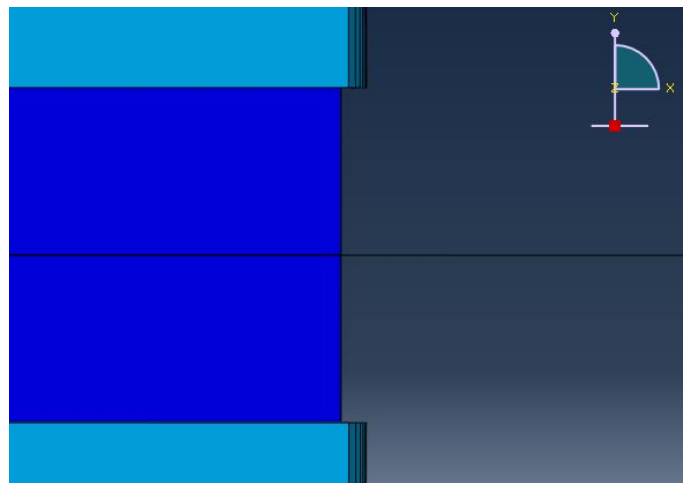


Figure 1: Clearance between Middle plate and Columns

In the figure above, the middle line here is the Middle plate, the dark blue element is the box and the light blue structural elements are the columns. It can be seen that there exists a clearance of 0.1 mm between Middle plate and the columns. But the value of this clearance has been passed to the solver as **zero**.

All the contact pairs have the same tangential and normal interaction. **Penalty** type frictional behaviour exists between the surfaces in contact. The coefficient of friction between these surfaces is  $\mu = 0.6$ . The type of normal contact used between the surfaces was **Linear** and the value of Contact Stiffness employed was  $10^8 N/mm$ .

### 3 Fracture modelling in B1PT0

Fracture modelling plays a great role in deciding the overall force displacement characteristics of B1PT0. Several simulation were done to identify the most appropriate fracture criterion such that minimum deviation from the experimental results are observed. In our model we have considered **ductile fracture** as the failure type for all the materials used in this simulation.

The fracture strain for this type of failure is found to be dependent on **Stress Triaxiality and Strain rate**. *It has been found through several experiments that the fracture strain decreases as the Stress Triaxiality increases.* Our model is undergoing static analysis so the strain rate is very small. Still the strain rate was recorded over the time period of the analysis at the locations which were vulnerable to fracture. These location were the corners of the contact region between columns and beams. At these location, the max value of the strain rate was found to be 0.00285.

In the experiments, cracks were observed in the weld which connected the floor beam and upper column. Because of this observation different fracture criteria has been assigned to different materials. Although the fracture was observed in only one region i.e. weld between floor beam and the column, other materials will experience stiffness degradation as the seismic load reaches 3% drift. Due to this reason, **Damage Evolution** was used along side **Ductile Fracture** criteria to incorporate the effects of stiffness degradation.

In order to obtain numerical force displacement behaviour close to the experimental one, trial and error was used to find the most appropriate fracture criteria and criteria for damage evolution. For this purpose nine simulations on B1PT0 were performed and out of those **nine** simulations, closer values and desired profile of force displacement curve were obtained for **three** simulation.

Before having a look at criterion, let's first look at the variables and parameters based on which these criteria are defined.

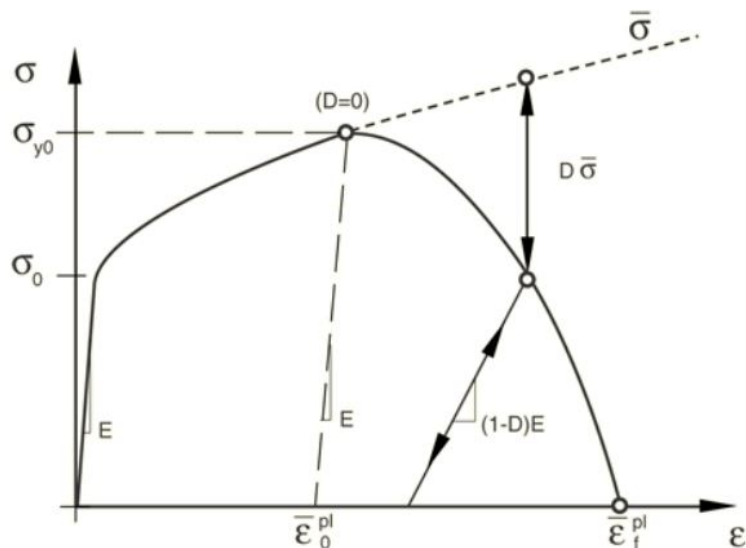


Figure 2: Stress-strain curve with progressive damage degradation

Here,

D is overall damage variable

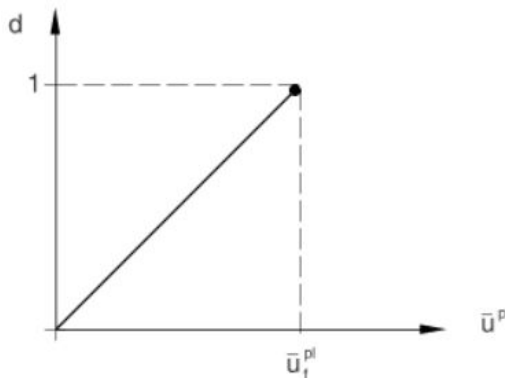
$\bar{\epsilon}_0^{pl}$  is the equivalent plastic strain at ultimate point which is the onset of fracture

$\bar{\epsilon}_f^{pl}$  is the equivalent plastic strain at the fracture point

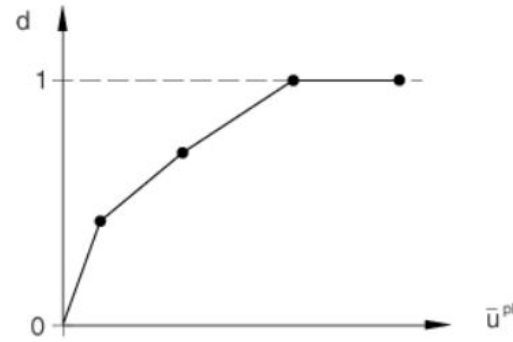
$\sigma_{y0}$  is the ultimate tensile strength

$\sigma_0$  is the yield stress

There is another very important variable known as effective plastic displacement,  $\bar{u}^{pl}$ . The evolution of  $\bar{u}^{pl}$  is given by  $\dot{\bar{u}}^{pl} = L \times \dot{\bar{\epsilon}}^{pl}$ . On integration, this equation will become  $\bar{u}_f^{pl} = L \times (\bar{\epsilon}_f^{pl} - \bar{\epsilon}_0^{pl})$ . L is the characteristic length of the element and in our case it is 8 mm for the beams and 20 mm for the column. In ABAQUS, the overall damage variable D is a function of  $\bar{u}^{pl}$ . In this simulation we have considered linear and tabular variation of D with respect to  $\bar{u}^{pl}$ . At  $\bar{u}^{pl} = \bar{u}_f^{pl}$ , the value of D = 1 and the corresponding element will be deleted from the simulation.



(a) Linear D vs  $\bar{u}^{pl}$



(b) Tabular D vs  $\bar{u}^{pl}$

The fracture and damage evolution criteria for the four simulations are given below:

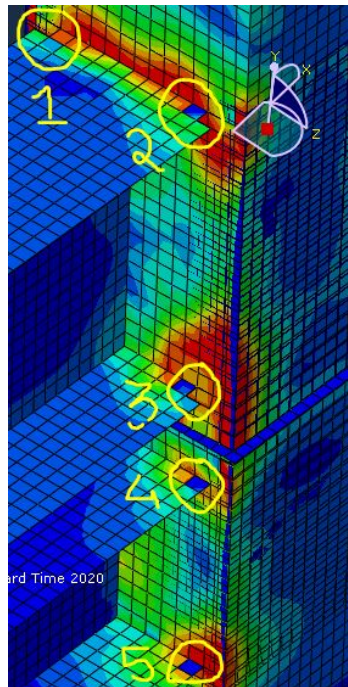
Fracture Criteria for Simulation 1			
Material	Fracture Strain	Stress Triaxiality	Strain Rate
Floor Flange	0.3	1	0.00285
Floor Web	0.3	1	0.00285
Ceiling Flange	0.3	1	0.00285
Ceiling Web	0.3	1	0.00285
Column	0.4	0.6	0.00285

The damage evolution criteria for all the materials were same for Simulation 1. Linear evolution with  $\bar{u}_f^{pl} = 0.7$  was used. Fracture and damage evolution criteria were not applied to Rod and Box.

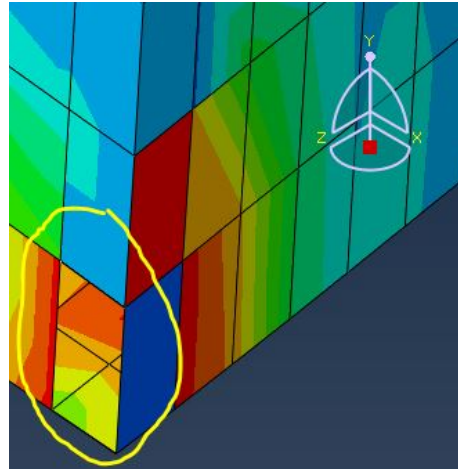
Fracture Criteria for Simulation 2			
Material	Fracture Strain	Stress Triaxiality	Strain Rate
Floor Flange	0.1	1	0.00285
Floor Web	0.3	1	0.00285
Ceiling Flange	0.1	1	0.00285
Ceiling Web	0.3	1	0.00285
Column	0.4	0.6	0.00285

The damage evolution criteria for all the materials except Column were same for Simulation 2. Linear evolution with  $\bar{u}_f^{pl} = 0.7$  was used. For Column, Tabular evolution was used as shown in table below. Fracture and damage evolution criteria were not applied to Rod and Box.

Damage Evolution Criteria for Column in Simulation 2	
D	$\bar{u}^{pl}$
0	0
0.5	0.5
1	2



(c) Element deletion from beams in Simulation 1



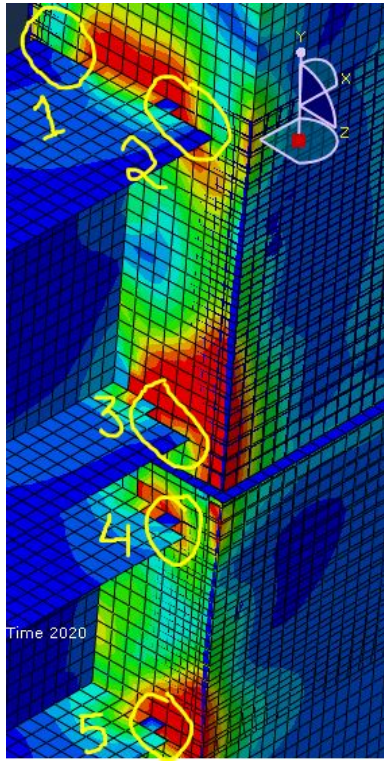
(d) Element deletion from column in Simulation 1

Fracture Criteria for Simulation 3			
Material	Fracture Strain	Stress Triaxiality	Strain Rate
Floor Flange	0.1	1	0.00285
Floor Web	0.1	1	0.00285
Ceiling Flange	0.3	1	0.00285
Ceiling Web	0.3	1	0.00285
Column	0.4	0.6	0.00285

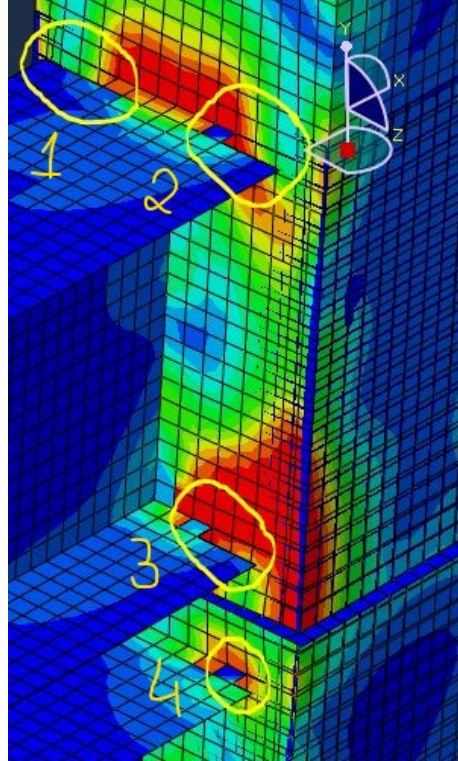
The damage evolution criteria for all the materials except Column and Ceiling Flange were same for Simulation 3. Linear evolution with  $\bar{u}_f^{pl} = 0.7$  was used. For Column, Tabular evolution was used as shown in table below. Fracture and damage evolution criteria were not applied to Rod and Box.

Damage Evolution Criteria for Column in Simulation 3	
D	$\bar{u}^{pl}$
0	0
0.5	2
1	8

Damage Evolution Criteria for Ceiling Flange in Simulation 3	
D	$\bar{u}^{pl}$
0	0
0.9	0.7
0.91	0.8
0.915	0.9
1	2



(e) Elements deleted from beams in Simulation 2



(f) Elements deleted in Simulation 3

In the first Simulation, it can be observed that element were deleted from the corners of the floor beam. There were no elements that were deleted from ceiling beam. Element deletion also took place from the column at the bottom of the structure. These deletion can be seen in figure (c) and (d). With these criteria, the value of forces obtained were higher than those found in experiments.

Some changes were made to the fracture and damage criteria in Simulation 2 in order to reduce the magnitude of forces obtained in Simulation 1. For this purpose the value of fracture strain for the flange material of floor and ceiling beam were reduced from 0.3 to 0.1. Also to avoid the element deletion in column, damage evolution criteria was modified and higher effective plastic displacement was used. With this modification, no elements were deleted from the columns. But it can be seen that elements were deleted from both the beam. Encircled location in figure (e) displays the deleted elements from the structure. This entire change in criteria, reduced the magnitude of force. The value of force at 3% drift in  $-\Delta$  direction was matching with the experimental value. But in  $+\Delta$  direction numerical force value was found to be lesser than the experimental value.

Some minor changes were made to the criteria in Simulation 3 which can be observed through table. These minor changes prevented the fracture to occur at location 5 in simulation 3. Still fracture were observed at the four locations in Simulation 3. Due to these fracture the value of forces did not increase much. A comparison of skeleton curves will be shown in the subsequent sections.

## 4 Planning the analysis for B1PT0

Planning the analysis into steps is an important aspect that should be considered especially for problems involving contact. This is recommended because to proceed with solving the effects of load on the model it is important that all the contact has been established between the contact surfaces. Hence we need to divide our analysis into two steps i.e. **Contact** and **Seismic Step**.

### Initial Step

In this step all the displacement boundary conditions are established.

### Step 1 - Contact

The time period of this step is 2 seconds. All the contact models are initialised in this step and their effect will propagate through the subsequent steps. Additionally, in this step the axial load, applied at the corners of upper end of the upper module, will increase linearly over the time period of this step to 100 kN establishing contacts between all the contact surfaces. Once the axial load reaches the 100 kN mark, this load value is propagated to the next step i.e. the **Seismic Step**.

### Step 2 - Seismic Step

The time period of this step is 4786 seconds. In this step, the seismic load will be applied up to 3% drift in both  $+\Delta$  and  $-\Delta$  direction. All the contact based output variables are active in this step.

With this plan, the analysis will proceed smoothly and there will be no errors related to modelling that can terminate the analysis.

## 5 Numerical results from Simulations on B1PT0

From the above sections it is clear that how the modelling was done, what features of ABAQUS were used and what values of necessary parameters were chosen to mimic the experimental response of B1PT0 under seismic load. In this section, force displacement characteristics i.e. skeleton curve along with energy dissipation curves will be used to display the results from simulations and simultaneously a comparison with the experimental results will be shown. Below is a table that contains the force displacement data for skeleton curve from both numerical and experimental response of the structure.

Force Displacement data				
Displacement in mm	Experimental	Simulation 1	Simulation 2	Simulation 3
100.24	13174.13	13751	10914.5	11314.3
63.22	11281.48	12562.72	11325.4	11329.2
49.88	9900	11300	10630.7	10630.7
32.43	7730.17	8863.47	8635.26	8635.26
24.54	7270.61	7411.69	6957.33	6957.33
16.64	6161.64	5280.28	4895.92	4895.92
12.39	4965.1	4233.61	3823	3823

Force Displacement data				
Displacement in mm	Experimental	Simulation 1	Simulation 2	Simulation 3
-12.08	-4727.73	-4374.93	-4192.44	-4192.44
-16.36	-6093.74	-5501.6	-5399.17	-5293.81
-24.98	-7409.34	-7712.06	-7534.18	-7534.18
-32.7	-8585.03	-9622.8	-9304.67	-9337.43
-49.8	-9902.45	-12210.5752	-11532.51758	-11532.96
-64.42	-11551.09	-13856.6	-11786.97	-12423.76
-98.90	-11000	-13609.89	-10680.38	-12105.40

The above data can be visualised in a better through the skeleton curve shown below.

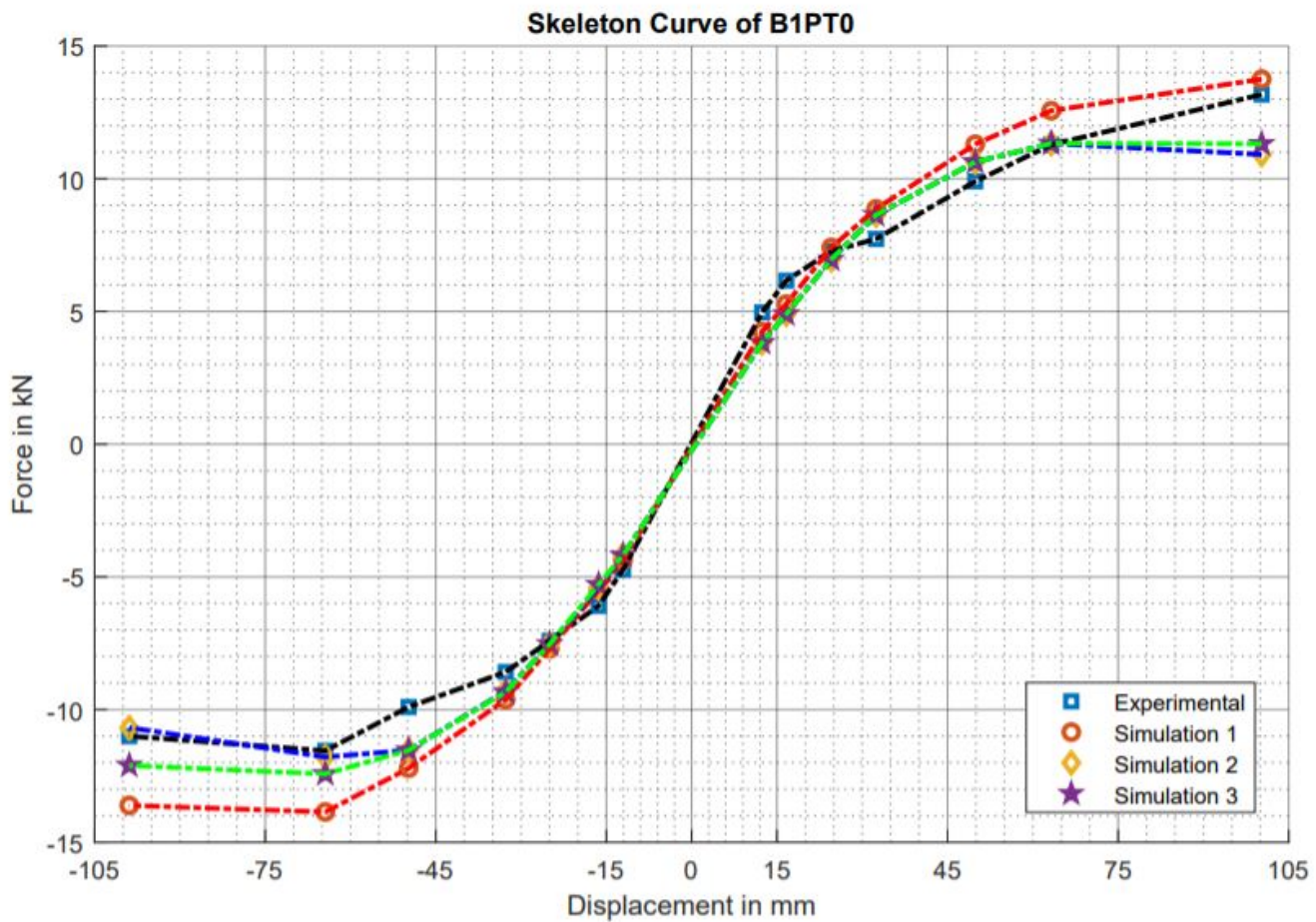


Figure 3: Skeleton Curve

One point that should be noted is that the slope of curve near 2% and 3% drift in simulation 1 is similar the experimental one. One issue that can be observed from the above curve is that the initial stiffness in simulation is less than the initial stiffness seen in experimental skeleton curve.

Energy dissipation in B1PT0 is predominantly observed due to plastic dissipation and frictional dissipation. Frictional dissipation occurs due to presence of friction between contact surfaces and at the end of the beam.

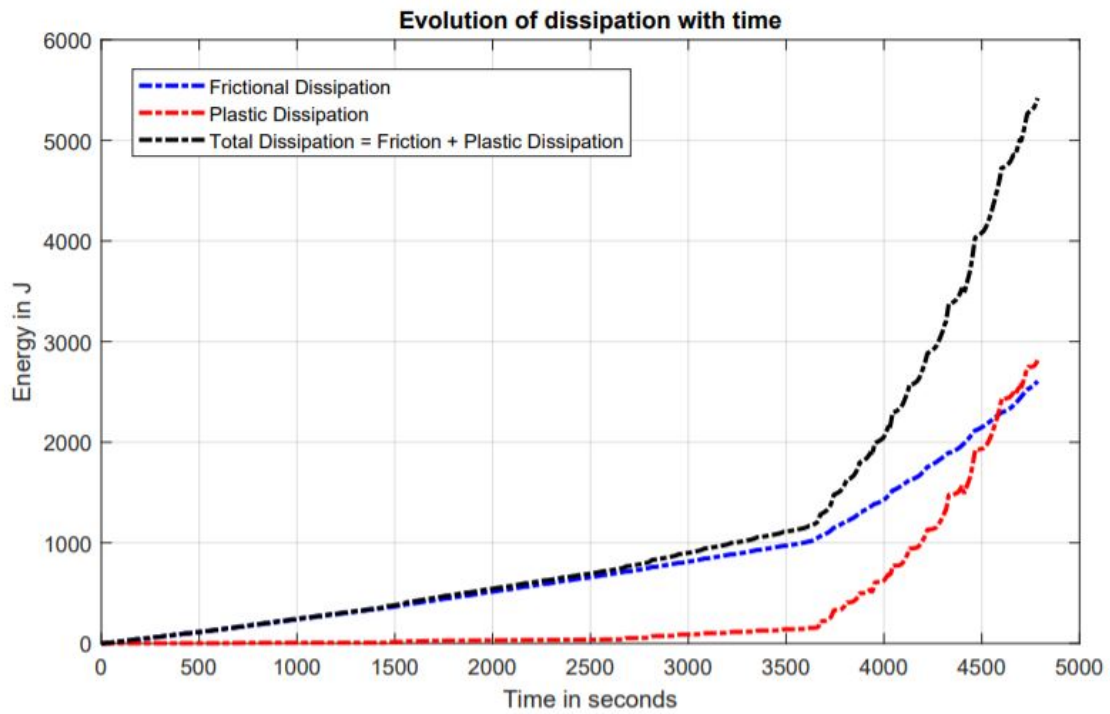


Figure 4: Evolution of Energy Dissipation with time

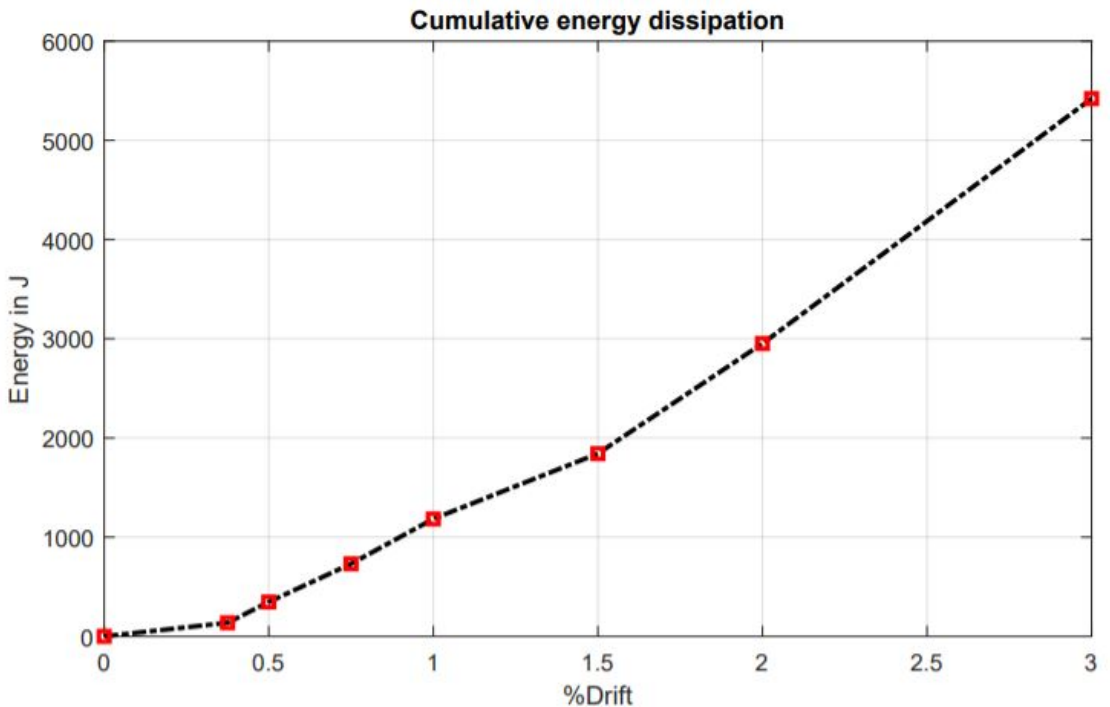


Figure 5: Cumulative energy dissipation VS %Drift